Oxygen consumption of bovine granulosa cells *in vitro*

A thesis presented in partial fulfilment of the requirement for the degree of

Master of Engineering

in

Biotechnology

at Massey University, Palmerston North,

New Zealand

Dongxing Li

2012

Abstract

The oxygen consumption rate of granulosa cells is considered to be a key determinant of oocyte oxygenation in follicles. The oxygen status of the oocyte potentially dictates its developmental competence. However, quantitative information on the oxygen consumption rate of granulosa cells in literature is scarce. This limitation has hindered further investigation into the oocyte oxygenation, which could potentially be used as an indicator for selecting high quality oocytes for producing high quality embryos. This could ultimately contribute to improvement of the success rates of human In-Vitro Fertilisation.

In light of this issue, this work developed a method for measuring the oxygen consumption rate of granulosa cells *in vitro*. This included techniques related to granulosa cell harvest from cows, suspending/culturing granulosa cells in culture medium and development of a competent respirometer. Each measurement run on the oxygen consumption rate of granulosa cells was conducted by suspending the granulosa cell culture in the respirometer, in which an optical-based oxygen sensor probe was employed to continuously monitor the oxygen partial pressure change in the cell suspension.

Five separate sets of respirometer data were collected and used to calculate the oxygen consumption rate, giving a range of 2.1 to 3.3 x 10^{-16}mol.cell^{-1}.s^{-1}/0.16 to 0.25mol.m^{-3}.s^{-1}. These rates were comparable with but higher than other animal cell oxygen consumption rates reported by the literature. They were approximately 5 times higher than the oxygen consumption rate of granulosa cells harvested from sheep (Gosden & Byatt-Smith 1986).

The implications of the measured oxygen consumption rate were then examined in the context of oxygen transport in large bovine preantral follicles via an existing mathematical model. The resulting predicted oxygen profiles in large bovine follicles were consistent with the study of Redding *et al.* (2007), which showed that as a preantral follicle grew the oxygen transport across the follicle was increasingly strained, resulting in subsequent decrease in oocyte oxygenation. By applying the bovine specific parameter estimates to the model, this work predicted that the largest follicle radius for the oxygen transport in bovine preantral follicle was 134µm, beyond which the oxygen could not reach oocyte. Since the experimentally reported sizes of the large bovine preantral follicles ranged of 58 to 145µm in radius (see Section 7.1.2), this work proposed that the oxygen transport was capable of oxygenating the oocytes in all but the largest preantral follicles. If bovine preantral follicles were to grow larger than they are experimentally observed to do so, all oocytes contained within such follicles would be in a hypoxic state. This is a result consistent with other work.

Furthermore, based on the use of bovine and ovine specific parameter estimates in the model, this work found that oxygen transport in follicles was likely to be the result of a unique combination of parameters for a particular species. Specifically the oxygen consumption rate and fluid voidage of follicles of a given species would be the key determinants in oxygen levels across the follicle. This work also found that the fluid voidage range across large bovine preantral follicles was reasonably wide (0.34 to 0.65) and the value increases with the follicle size. This suggested that the use of fluid voidage for investigating the oxygen levels across

preantral follicles must be follicle size specific. Finally, this work presented a nomograph which described the relationship among fluid voidage, follicle radius and oxygen levels at oocyte surface. The nomograph can be used as a tool for further research to study the oxygen status of the oocyte during the growth of a large bovine preantral follicle and may be generalised to describe non-species specific follicle oxygenation in growing follicles.

Acknowledgements

Many thanks to my supervisors, Dr. Gabe Redding and Dr. John Bronlund. Gabe, thank you for teaching me logical thinking and spending considerable amount of time editing my thesis. Your wise idea and correction on my thesis really help me a lot. Thank you for taking me to the abattoir and show me how to cut ovaries from cows post mortem. John, thank you for letting me do this project in spite of that trouble I caused at the lab. Thank you for teaching me oxygen uptake kinetics and how to use Excel to analyse the data. Thank you for solving the crisis, in which I was almost forced to leave New Zealand. Thanks also to Colin Brown for enlightening the respirometer design.

Many thanks to Affco New Zealand Ltd. Thanks for allowing us to collect ovaries.

Many thanks to all staff in Institutes of Technology & Engineering Micro Suite. Ann-Marie Jackson, thank you for your help and tolerance.

Dad, Mum, thank you for your support.

Table of Contents

Chapter 1. Introduction

It is well accepted that oxygen plays a crucial role in ovarian follicular development. Oxygen is an essential nutrient for the metabolism of granulosa cells, and also for the metabolic pathway of the oocyte.

The mathematical model developed by Gosden & Byatt-Smith (1986) showed that in preantral follicles, the centrally located oocyte might be hypoxic due to severe oxygen depletion by the granulosa cells which surrounded it. This possibility of intrafollicular hypoxia has generated interest among researchers.

Due to the difficulties of directly measuring the intrafollicular oxygen content *in vivo*, mathematical modelling has been employed as a tool to predict the oxygen levels across follicles (Gosden & Byatt-Smith 1986; Clark *et al.* 2006; Redding *et al.* 2007, 2008). Based on the model proposed by Gosden & Byatt-Smith (1986), Redding *et al.* (2007) developed a similar mathematical model and showed that as preantral follicle grew oxygen transport across the follicles became increasingly strained. Eventually, oxygen transport reached a maximum-strain point as the follicle grew up to a threshold size beyond which the oocyte in the follicle would inevitably suffer hypoxia. The consensus of the previous two studies on intrafollicular hypoxia raised an interesting question. How does the follicle overcome this apparent oxygen transport limitation so that it can continuously deliver oxygen to the oocyte as the follicle grows beyond the threshold size at which further growth will result in the hypoxia?

Oxygen transport limitation is underlain by the oxygen consumption rate of granulosa cells. To a large extent, the conclusions regarding intrafollicular hypoxia in the previous studies were inferred based on the magnitude of the oxygen consumption of the granulosa cells (Gosden & Byatt-Smith 1986; Redding *et al.* 2007). However, quantitative information on the oxygen consumption rate of granulosa cells is sparse. To our best knowledge, a quantitative measure of the oxygen consumption rate of granulosa cells has only been reported by Gosden & Byatt-Smith (1986). Furthermore, the reported value represented a single value; no repetitive measurement was carried out and the methodology was lacking details of how the value was obtained. The limited information in the literature has resulted in this value being repetitively used by subsequent studies on investigating the oxygen transport across the follicle. In order to substantiate or otherwise the findings of subsequent research which has relied on this single value it is important to obtain further experimental measurements of this parameter so that the likely limits of its true magnitude can be established with greater confidence. Furthermore, whether or not granulosa oxygen consumption varies among mammalian species is also unknown.

Thus, this work aims to focus on obtaining a series of new data on the oxygen consumption rate of the granulosa cells for investigating the oxygen transport across follicles in further studies. Without this information the progress of research regarding intrafollicular oxygen

content may be hindered by the limited information on the oxygen consumption rate of granulosa cells.

To measure the oxygen consumption rate of granulosa cells, the experimental work carried out will need to focus on techniques for handling somatic cells, as well as those for measuring oxygen consumption rates in such cells. Previously, the oxygen consumption rate of ovine granulosa cells was measured with a polarographic oxygen electrode probe by Gosden & Byatt-Smith (1986), who subsequently proposed the concept of intrafollicular hypoxia for the first time. With the progress of technology since 1986, the optical oxygen sensor has superseded the oxygen electrode for measuring the cellular oxygen consumption rate. This new technique allows the oxygen consumption rate of cells to be monitored with good precision and is much more robust than many systems which were commonly used in the past. Moreover, abundant studies involving granulosa cell harvest and culture have been conducted since 1986, which provide a wealth of both quantitative and empirical information on handling granulosa cells and follicles.

The objective of this work is to quantify the oxygen consumption rate of granulosa cells and subsequently use this data as input into existing mathematical models to further examine oxygen transport limitations in follicles. Bovine granulosa cells will be studied due to their availability at a local abattoir.

In order to achieve these objectives, a detailed review of granulosa cells and the experimental methods for granulosa cell harvest is carried out in the next chapter (Chapter 2). Existing techniques for measuring cellular oxygen consumption rates will be reviewed in Chapter 3 which subsequently describes the design of preliminary respirometer for use in this work.

Chapter 2. Literature review

The objectives set out in Introduction require the oxygen consumption rate of granulosa cells to be measured. To achieve this, basic knowledge of the granulosa cell function and the techniques for granulosa cell harvest and culture are essential. This chapter will therefore focus on reviewing available literature in these key areas.

2.1 Ovaries and follicles

In order to harvest granulosa cells, knowledge of the location of granulosa cells *in vivo* is important. Granulosa cells reside in the internal walls of follicles that grow in ovaries (Figure 2.1; 2.2).

Figure 2.1 depicts the location and shape of human ovaries *in vivo*; the shape and size of an ovary resembles an almond. In the ovary (Figure 2.1, right), the different follicle development stages can be distinguished based on the cross sections of the follicles.

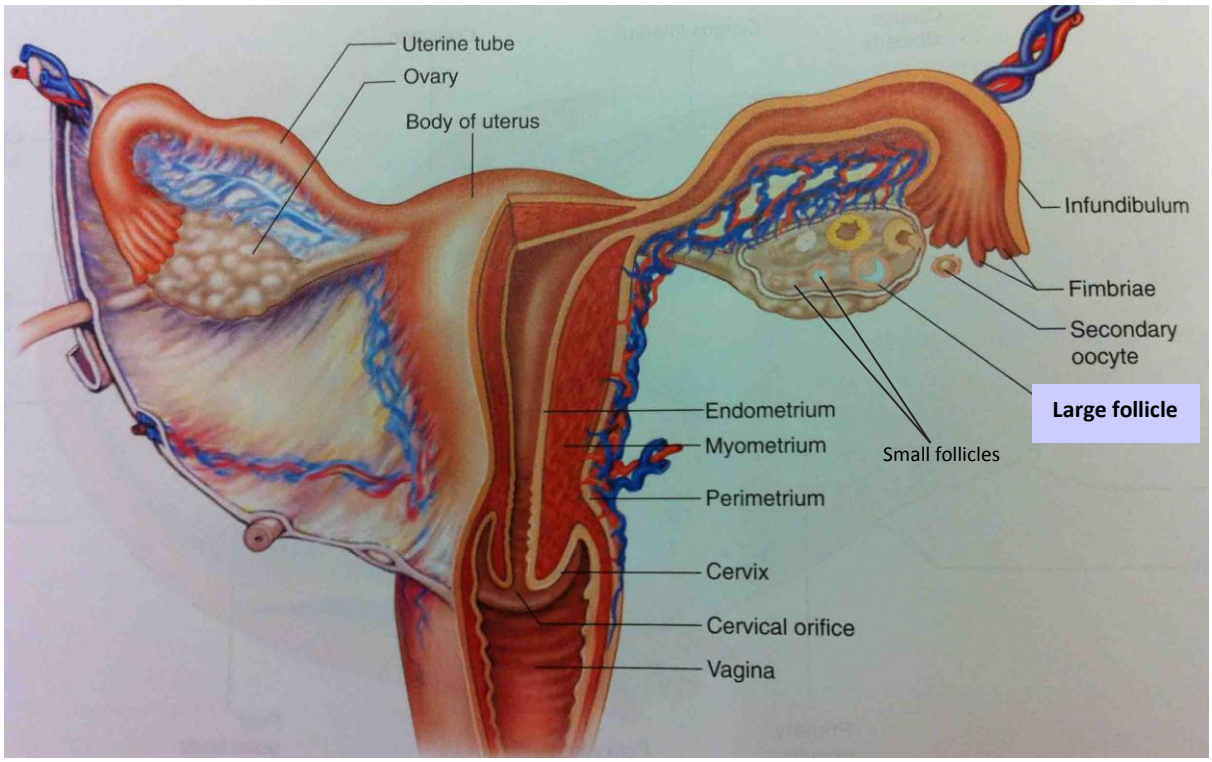

Figure 2.1 Structure of a human female reproductive system (Image taken from Shier *et al.* 2006).

An ovary contains numerous follicles, each of which will be in various stages of development. A basic description of the developmental stages of a follicle and location of granulosa cells is depicted in Figure 2.2.

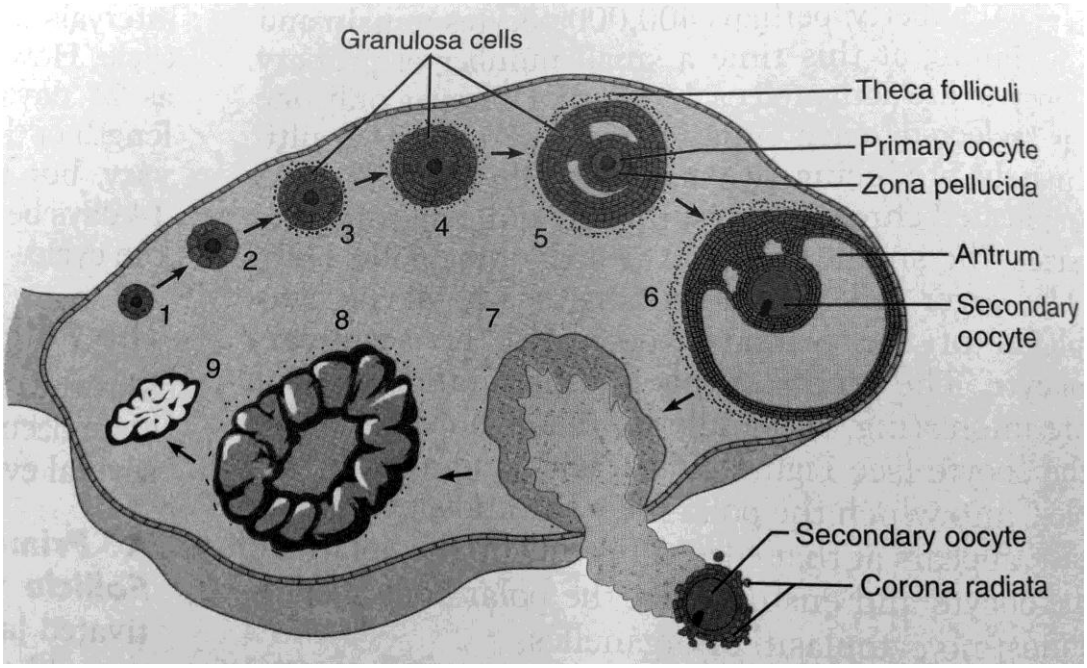

Figure 2.2 Schematic views of the developmental stages of a follicle. Where depicted numbering describing the following, 1. The primordial follicle; 2. The small preantral follicle; 3. The growing preantral follicle; 4. The large preantral follicle; 5. The early antral follicle; 6. The dominant follicle; 7. The ruptured follicle; 8. The corpus luteum; 9. The scarlike corpus albicans (Image taken from Marieb 2004).

Follicular development occurs as part of the menstrual cycle, during which follicles within the ovary mature. Starting as a primordial follicle (Picton *et al.* 1998; Juengel *et al.* 2002), a follicle may mature through the various stages of follicle development to a dominant follicle (shown by Figure 2.2, step 1-6), after which ovulation may occur (shown by Figure 2.2, step 7). The maturation of a follicle in a human ovary requires almost one year (Gougeon 1986). The majority of growing follicles do not fully complete this maturation; instead, they undergo an apoptotic process, known as atresia. Typically, one or sometimes two follicles may proceed through to ovulation in any given menstrual cycle (Gougeon 1996).

2.2 Development of the follicle and its follicular cells in each follicular stage

This section describes each of the follicular developmental stages in detail as they relate to the granulosa cells and oocyte contained within the follicle.

The follicular cross-sections shown in the figures below are derived from different mammals. However, the general features of mammalian follicles are known to be remarkably similar between species. Typically, the follicles are roughly spherical and are composed of granulosa cells and an oocyte. The space between the granulosa cells is filled by the follicular fluid. The coalescence of this fluid into a fluid antrum is also a defining common feature.

2.2.1 Primordial follicles

In an ovary, the mitotic division of primordial germ cells result in the formation of oogonia. Gradually, the oogonia are surrounded by somatic cells which are called the cortical cords. Within the cords, oogonia undergo DNA replication to enter meiosis and become oocytes (Van den Hurk & Zhao 2005). An oocyte and associated epithelial tissue derived from the cortical cord compose the earliest form of an ovarian follicle, known as a primordial follicle. The epithelial cells are known as pre-granulosa cells. Primordial follicles are considered the female fundamental reproductive units and are the most abundant of all follicle types within an ovary. The maximum number of primordial follicles in a human ovary can reach 7 million. These primordial follicles are quiescent until they are recruited into the follicular development cycle or undergo the process of apoptosis directly (Clark 2008).

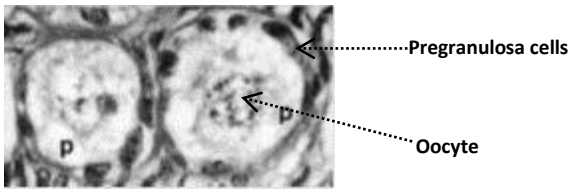

Figure 2.3 Cross-sections of two primordial follicles (marked by **P**; taken from a cow ovary). Where the pregranulosa cells and oocyte are indicated by arrowheads. (Image taken from Braw-Tal & Yossefi 1997).

At this earliest follicular stage, an oocyte is surrounded by one layer of flattened pregranulosa cells. The primordial stage is the longest developmental stage of any of the stages of follicular development, lasting over 150 days in human (Gougeon 1986).

2.2.2 Primary follicles

The follicle develops into a primary follicle as the pregranulosa cell layer thickens and the cells become cuboidal (Figure 2.4). The oocyte also increases in diameter. The epithelial cells which surround the oocyte are now known as granulosa cells (Salha *et al.* 1998).

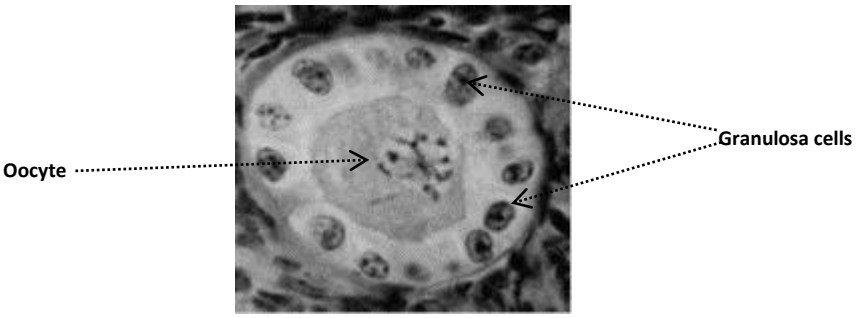

Figure 2.4 A cross-section of the primary follicle (taken from a cow ovary). Where the granulosa cells and the oocyte are indicated by arrowheads (Image taken from Braw-Tal & Yossefi 1997).

2.2.3 Early preantral follicles

As the granulosa cells proliferate, two or more layers of the granulosa cells are formed and surround the oocyte. At the same time, loose connective tissue emerges at the outmost granulosa cell layer and encases the whole follicle. The cells which compose this tissue are known as thecal cells. These new features characterize that the follicle has moved into the early preantral stage of follicular development (Figure 2.5).

In addition, during this follicular stage, a basement membrane forms between the granulosa layer and thecal layer. At the same time the zona pellucida, a glycoprotein membrane derived from secretion of the oocyte, forms between the oocyte and granulosa layer (Van den Hurk & Zhao 2005) (Figure 2.5).

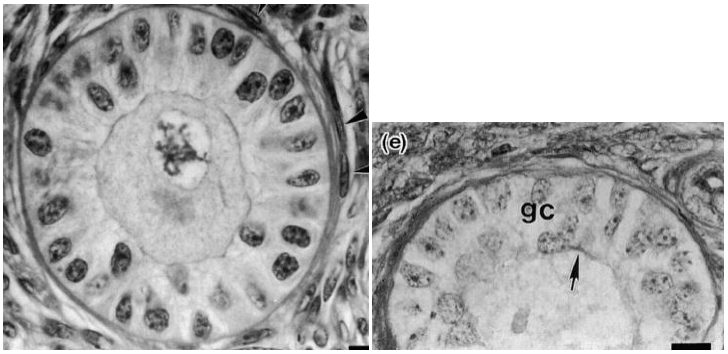

Figure 2.5 A cross-section of the preantral follicle in the early stage of development (taken from a cow ovary; left image). The right image marks the zona pellucida (arrow) and granulosa cell layer (gc) (Images taken from Braw-Tal & Yossefi 1997).

2.2.4 Late preantral follicles

Figure 2.6 shows a cross-section of the late preantral follicle. At this stage, the oocyte becomes larger and is surrounded by approximately five granulosa cell layers. The space between the granulosa cells is filled by follicular fluid which is derived from serum and granulosa cell secretion (Clark 2008).

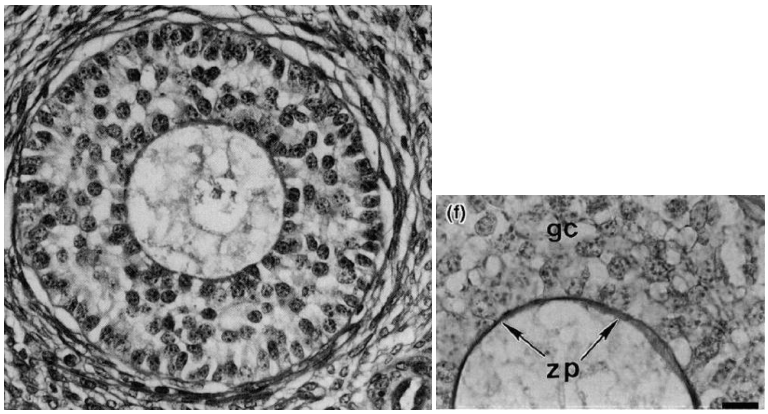

Figure 2.6 A cross-section of the late preantral follicle (taken from a cow ovary; left image) and Zona pellucida (zp) (arrows; right image) (Images taken from Braw-Tal & Yossefi 1997).

2.2.5 Early antral follicle

As small pockets of follicular fluid appear between the granulosa cells, an early antral follicle forms (Figure 2.7).

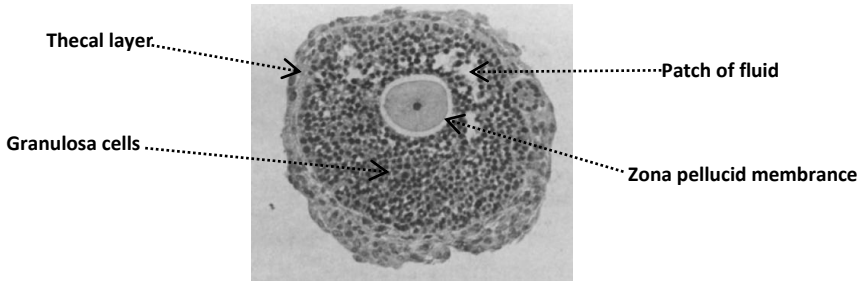

Figure 2.7 A cross-section of the early antral follicle (taken from a rat ovary). Where discrete pockets of follicular fluid, the thecal layer, granulosa cells and zona pellucid are indicated by arrowheads (Image taken from Boland *et al.* 1993).

2.2.6 Antral follicle

As the follicle grows the discrete pockets of follicular fluid coalesce into a common cavity which characterizes the follicle as having progressed to the antral follicular stage (Figure 2.8).

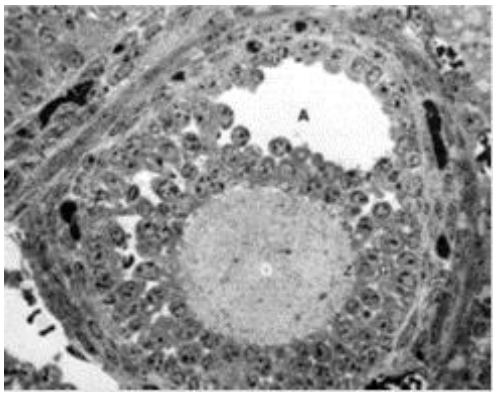

Figure 2.8 A cross-section of an antral follicle (taken from a cat ovary). Where the antrum filled by follicular fluid is labeled with **A** (Image taken from Moran & Rowley 1988).

2.2.7 Dominant follicle

Figure 2.9 depicts a cross-section of the late antral follicle, also known as a dominant follicle.

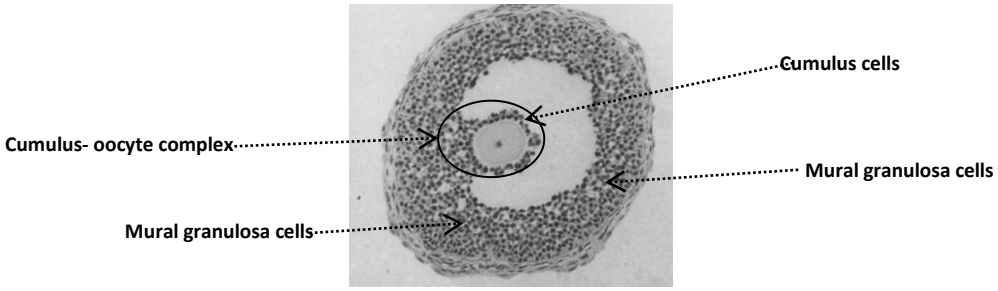

Figure 2.9 A cross-section of the dominant follicle (taken from a rat ovary). Where, the cumulus-oocyte complex is circled, and the cumulus and mural granulosa cells are indicated with arrowheads (Image taken from Boland *et al.* 1993).

In this follicular stage, the oocyte with its surrounding granulosa cells projects into the antrum and forms a hillock known as the cumulus- oocyte complex (Figure 2.9). The granulosa cells are differentiated into two distinct subtypes, namely, mural granulosa cells and cumulus cells. Cumulus cells are coupled with the oocyte and mural granulosa cells are associated with follicular wall (Li *et al.* 2000).

2.3 Vascularisation and oxygen transport in follicles

The supply and removal of substances from the follicle is believed to be largely dictated by the extent of the vascular network at the follicular surface. Van Blerkom *et al.* (1997) have shown this to be the case for intrafollicular oxygen content, with follicles with higher degrees of vascularisation exhibiting higher oxygen levels.

Initially, an early primordial follicle does not possess an independent capillary network, and it relies on the stromal vessels which are nearby to obtain nutrients. Soon after, an initial vascular supply which may be composed of only one or two arterioles is developed in the later primordial follicle. As the arterioles develop, a complex capillary network is formed. A fully grown vascular network will form in the theca layer as the follicle grows into the antral stage (Geva & Jaffe 2000).

The capillaries at the follicular surface do not penetrate the basement membrane which exists between the theca layer and the granulosa cell layer; thus, the internal follicle environment is avascular. Nutrients are transported into follicles by diffusion that relies on the permeability of the capillaries and basement membrane. Key nutrients for follicular growth include oxygen, growth factors, hormones, glucose, electrolytes, and enzymes (Avery *et al.* 2003). Oxygen is a small molecule and it can easily diffuse through both the basement membrane and the membranes surrounding follicular cells such as granulosa cells. Large molecules such as

glucose are carried into granulosa cells via transporter proteins located in the follicular cell membrane (Clark 2008).

Oxygen is consumed by granulosa cells as it diffuses through the granulosa layer. The mathematical model of Gosden & Byatt-Smith (1986) predicted that the majority of oxygen was consumed in the outer granulosa cell layers, leaving the internal layers and oocyte in a state of hypoxia. Redding *et al.* (2007) proposed that oxygen transport in granulosa layer should account for the follicular fluid between cells (see Section 2.2.4) in which the oxygen transport was easier as no oxygen was consumed. Furthermore, the follicular fluid among granulosa cells increases as the preantral follicle grows, which gradually facilitates oxygen transport. This is counteracted by the increasing number of cells and increased diffusion distances as the follicle grows. Mathematical prediction showed that the balance between these factors made it possible for the oocyte to still receive oxygen as the follicle grew, however transport to the oocyte became marginal in the late preantral phase. Thus, follicular fluid was deemed to be an important factor for facilitating mass transport in follicle.

2.4 Effect of intrafollicular factors on granulosa cells

Granulosa cells are affected by two factors *in vivo*, which are the paracrine factors and the factors derived from the follicular wall. Paracrine factors are secreted by oocytes. Proliferation of granulosa cells is controlled by paracrine factors (Li *et al.* 2000). The factors derived from follicular wall include various nutrients which diffuse through the follicle from the capillary network in the theca layer. Granulosa cells rely on these nutrients to grow.

The role of oocyte-secreted paracrine factors in regulating metabolic activities and differentiation of granulosa cells has attracted considerable research attention (reviewed by Sugiura & Eppig 2005). During the early follicular stages, the oocyte is growing and the paracrine factors secreted by the growing oocyte does not affect granulosa cell metabolism. However, the paracrine factors have been shown to control the metabolism and phenotype of the granulosa cells once the oocyte is fully grown. The completion of oocyte development always coincides with antrum formation in the follicle (Li *et al.* 2000; Sugiura *et al.* 2005). The regulation of paracrine factors results in increased granulosa cell metabolic activity and the appearance of the cumulus cell phenotype. However, the paracrine factors can only regulate the granulosa cells which are adjacent to the oocyte. The granulosa cells which are not affected by the paracrine factors present with the mural granulosa cell phenotype. Thus, the paracrine factors secreted by a fully grown oocyte differentiate the granulosa cells into two subtypes of cells: cumulus cells and mural granulosa cells.

The cumulus cells and mural granulosa cells play different roles in an ovarian follicle. The oocyte relies on the metabolic activities in the cumulus cells to break down some nutrients and produce the metabolites for growth of the oocyte (Donahue & Stern 1968; Leese & Barton 1985). The functionality of the mural granulosa cells is to facilitate primary endocrine function and assist the growth of an ovarian follicle. For instance, mural granulosa cells promote the upregulation of cumulus cells (Eppig *et al.* 2005; Sugiura & Eppig 2005). Furthermore, Clark *et*

al. (2006) mathematically predicted that cumulus cells depleted oxygen at a relatively low rate which allowed for greater oxygenation of the oocyte. Thus, the oxygen consumption rate of cumulus cells may be much slower than the rate of mural granulosa cells.

2.5 The techniques of granulosa cell harvest

In order to study granulosa cells *in intro*, the cell isolation from surrounding tissue is important. The most common source of granulosa cells for harvest comes from ovaries collected from an abattoir. Previous literature describes many related techniques for granulosa cell harvest. This information is reviewed here so that it can be distilled into a suitable technique for the purposes of this work.

2.5.1 Ovary transportation and treatment

In this work, bovine ovaries will be used, which will be collected at an abattoir. A review on ovary transportation and treatment in a laboratory is presented below.

Most studies suggest that time between ovary collection and transportation to the laboratory should be less than two hours. Generally, bovine ovaries are put into 0.9% warm (30–35°C) saline in a thermally insulated flask (Nandi *et al.* 2008; Cetica *et al.* 2002; Sutton *et al.* 2003; Li *et al.* 2000). Alternatively, ovaries are placed in an ice-cold buffered salt solution (or cold PBS at 4°C) for transport. Granulosa cell viability tests show that this chilled condition does not affect the viability of the granulosa cells (Yada *et al.* 1999; Basini *et al.* 2004; Kotsuji *et al.* 1990; Basini & Tamanini 2000). Furthermore, Orsi *et al.* (2005) proposed that transporting ovaries in cold conditions could slow down the metabolism of ovarian cells; thus, the build-up of the products of metabolism caused by the absence of vascularisation to remove them would be reduced.

Ovaries are often washed with penicillin and streptomycin in the laboratory (Cetica *et al.* 2002). Alternatively, normal saline can also be used for washing (Nandi *et al.* 2008).

2.5.2 Isolation of follicles

Granulosa cells are located internally within the follicle. In order to harvest granulosa cells it is often useful to first isolate individual follicles from ovaries.

Telfer (1996) summarized current techniques used for follicular isolation from ovaries (Table 2.1).

Isolation method	Species	Follicle Sizes (μm)	Number of follicles per ovary
Collagenase+microdissection	Porcine	100-250	100
Mincing+Trypsin	Porcine	100-300	>100
Mincing+collagenase	Porcine	<60	>200,000
Mechanical grating device	Bovine	40-100	300
Tissue chopper with Successive filtration	Bovine Fetal Bovine calf Bovine cow	40-100	357 64 37
Micro dissection	Bovine	120-220	50

Table 2.1 Classification of the techniques for isolating the follicles from ovaries (Telfer 1996)

Normally, the method for isolating big follicles from bovine ovaries is to halve the ovaries by a scalpel first so that the follicles in the ovaries can be seen. The follicles are isolated from the surrounding connective tissue with scissors (Hamberger *et al.* 1971).

A follicle is considered healthy when it has a vascularised surface which is characterised by a pink or red colour and the follicular fluid is a clear amber colour with no debris (Yang & Rajamahendran 2000). Furthermore, the magnitude of vascularisation at the follicular wall and integrity of the follicular wall are also associated with healthy follicles. These characteristics can be examined under a stereomicroscope (Nandi *et al.* 2008).

2.5.3 Granulosa cell harvest

According to previous literature, two approaches are widely used for granulosa cell harvest.

The first approach is to use a syringe to puncture the follicle and aspirate the follicular fluid. The granulosa cells are sucked out along with the follicular fluid. Any debris and oocytes in the collected follicular fluid are then discarded with a micropipette under a stereomicroscope. The granulosa cells in the collection medium are harvested by centrifugation (600-800g for 3-5 minutes) (Kotsuji *et al.* 1990; Sutton *et al.* 2003; Li *et al.* 2000; Eppig *et al.* 1997; Van Blerkom *et al.* 1997; Basini & Tamanini 2000).

Alternatively, the follicle is cut and inverted. The granulosa cells are then scraped from the internal surface of the follicular wall into the collection medium by using the back of a scalpel blade or a plastic inoculation loop to sweep the intrafollicular wall. Afterwards, the isolated granulosa cells are harvested with a micropipette. The sweeping motion on the intrafollicular wall needs to be somewhat gentle; otherwise, the vessels in the thecal layer may be ruptured and the collection medium may be contaminated by blood (Hamberger *et al.* 1971; Allegrucci *et al.* 2003).

As described above, follicles are surrounded by a vascular network. Sometimes, the capillaries are ruptured as the granulosa cells are collected. The most common method of avoiding blood contamination is simply to discard those samples which visibly contain blood. However, frequent discarding in this manner result in a shortage of the cells. Thus, some studies treated the granulosa cells with 0.9% prewarmed ammonium chloride at 37°C for 1 min (Basini *et al.* 2004; Basini & Tamanini 2000) or 50% Percoll to remove blood from the granulosa cell collection (Pawshe *et al.* 1998).

The quantities of granulosa cells harvested from mammalian follicles are very limited on a per follicle basis. The maximum volume of granulosa cell suspension (cells plus culture medium) recorded in the literature is only 2ml (Gosden & Byatt-Smith 1986). Thus, research involving granulosa cells are conducted on a small scale; this appears to be common to all studies.

2.5.4 Granulosa cell culture

This work aims to measure the oxygen consumption rate of granulosa cells as they are suspended in culture medium. The culture medium must be capable of suitably sustaining the metabolic activity of the granulosa cells.

2.5.4.1 Granulosa cell culture medium and temperature

Most commonly, granulosa cells are suspended and cultured in Medium 199 (Basini *et al.* 2004; Metcalf 1982; Eppig *et al.*1997; Sutton *et al.* 2003; Gosden & Byatt-Smith 1986; Li *et al.* 2000; Pawshe *et al.* 1998).

However, a variety of other mediums have also been used. For example, a medium, which is composed of Waymouth's MB, Hanks' solution and fetal calf serum, was used by Yada *et al.* (1999) and Kotsuji *et al.* (1990). WAY/BSA/ITS was used by Vanderhyden *et al.* (1992). DMEM-F12 was used by Allegrucci *et al.* (2003). DMEM/Ham's F12 (1:1) was used by Basini & Tamanini (2000) and Van Blerkom *et al.* (1997).

The temperature for culturing granulosa cells is 37°C, and appears to be common to all studies.

2.5.4.2 Granulosa cell quantity and viability assessment

The quantity of viable granulosa cells is important for assessing the oxygen consumption rate of granulosa cells, since only viable cells contribute to this consumption. Hence, this work will need to quantify the number of viable granulosa cells in any given cell suspension.

In general, the viable granulosa cell count is determined by the following procedure.

Firstly, the cell viability is examined by mixing the granulosa cell suspension with the equivalent volume of 0.4% Trypan blue solution. The mixture is then placed into a water bath at 37℃ for 4 min, in which time the dead cells are stained to dark blue. Next, the viable cell concentration in the mixture is assessed by pipetting the sample from the mixture to a haemocytometer. Under a microscope, the viable granulosa cells in the grids of the haemocytometer are visualized and subsequently used to estimate the proportion of viable cells in the suspension (Basini *et al.* 2004; Yada *et al.* 1999; Allegrucci *et al.* 2003; Basini & Tamanini 2000; Kotsuji *et al.* 1990).

2.6 Conclusion

This review summarised basic knowledge of granulosa cells which will facilitate the development of a suitable method to harvest and culture the cells. This information will form the basis of some of the methodologies developed and described in the remaining chapters of this work.

This work aims to measure the oxygen consumption rate of granulosa cells in culture. Therefore, having examined culture techniques in this chapter, the next chapter will examine the development of the methodology associated with the measurement of cellular oxygen consumption.

Chapter 3. Preliminary respirometer design

This work aims to determine the oxygen consumption rate of granulosa cells in culture suspension. Unless otherwise stated consumption rates will be expressed in the form of mol/cell/s. This represents the oxygen consumption rate per viable cell.

The techniques for assessing viable cell number and the culture conditions for suspending granulosa cells have been well-established by previous studies (see Section 2.5.4.1; 2.5.4.2). The objective of this work is to develop a respirometer capable of monitoring the real-time change in the dissolved oxygen content in the granulosa cell suspension so that the dissolved oxygen depletion in the cell suspension over time can be measured.

In order to produce valid data on the oxygen consumption rate of granulosa cells via such measurement, this work requires that the measurement is conducted in the specific culture conditions capable of sufficiently sustaining the cells. These conditions will be introduced and discussed in the first part of this chapter. To fulfil the functionality of the respirometer, a suitable technique for real-time monitoring dissolved oxygen content in aqueous solutions is also required. Thus, the literature regarding the oxygen measurement methods as well as use of these techniques for measuring the oxygen consumption rate of mammalian cells will be reviewed as subjects in this chapter. Finally, based on the knowledge drawn up from the methodology review and the specific culture conditions for granulosa cells, a preliminary respirometer will be designed and constructed. Subsequent testing of the respirometer will also be carried out to determine its performance relative to the requirements of this work.

3.1 Specific culture conditions suitable for the measurement of granulosa cell oxygen consumption rate

Based on the literature review, this work has acknowledged two facts regarding the granulosa cell culture *in vitro*. Firstly, granulosa cells can be cultured in standard mediums which are capable of supplying essential nutrients for the metabolism of granulosa cells at 37°C (see Section 2.5.4.1). Secondly, the harvested granulosa cell number is limited (Section 2.5.3); thus, the volume of granulosa cell suspension for the measurement will be small.

In addition to these factors, to measure the oxygen consumption rate of granulosa cells, some other specific conditions must be achieved.

Firstly, the culture must be conducted in air tight conditions to ensure that the only cause of change in dissolved oxygen content in the granulosa cell suspension is due to the respiration of the granulosa cells.

Next, in order to assess the rate of oxygen consumption per cell, the number of cells which contribute to the oxygen depletion in the measurement must be determined. This work will assess the viable cell quantity by cell count after measurement of oxygen depletion. In order for this to be valid, the viable cell count should be the same at the beginning and end of the

measurement of oxygen depletion (i.e. cell death and/or proliferation must not change the viable cell count significantly over the time course of the measurement). In addition to this requirement the granulosa cells must be sufficiently dispersed to facilitate counting by visual observation.

Finally, this work requires that each granulosa cell experience essentially the same culture conditions. This requirement can be achieved by evenly distributing the granulosa cells in culture and ensuring that the culture is sufficiently mixed.

Given the requirement for a technique suitable for monitoring the oxygen content of cell culture, the next section reviews available techniques to determine their suitability for incorporation into the proposed system.

3.2 Review on the methodology for assesseing/monitoring dissolved oxygen content in aqueous solutions and measuring the oxygen consumption rate of mammalian cells

The techniques for analysing dissolved oxygen content in aqueous solutions are the basis of measuring the oxygen consumption rate of cells suspended in culture medium. Therefore, this is one of the key functionalities of the respirometer which this work aims to design and build. According to the literature, these techniques can be classified into four categories, which are titrimetric, manometric, amperometric, and optical techniques. In order to choose a suitable technique, these techniques are described in this section in an order reflecting their first description in the literature (oldest to newest).

3.2.1 Titrimetric analysis

Titrimetric analysis is the oldest technique for measuring the dissolved oxygen content in aqueous solutions (reviewed by Hitchman 1978). The basic principle of the technique is to fix the dissolved oxygen in the aqueous sample with $MnSO_4$ and KI. As a result of oxygen fixation, a brown precipitate ($Mn(OH)_3$) is formed. By titrating the $Mn(OH)_3$,the dissolved oxygen can be assessed.

Whilst this technique is potentially extremely accurate, it relies on a high degree of skill on the part of the operator and is also subject to a wide range of potential interferences, such as various ions and compounds in the aqueous sample.

The main advantage of titrimetric analysis is the ability to measure oxygen concentration directly. Other techniques typically measure the partial pressure of oxygen, which requires further knowledge of the oxygen solubility in the measurement medium if it is to be converted to concentration.

Since its first description in 1888 this technique has not been widely used in biological systems to continuously monitor dissolved oxygen levels. This is likely due to the fact that application of the technique results in at least partial destruction of the sample. The volume of granulosa cell suspension will be small; hence, sample destruction is likely lead to severe complications. This, combined with the fact the method requires significant operator skill and is subject to much interference make this method unsuitable for this work.

3.2.2 Manometric technique

The manometric technique was first reported by Barcroft & Haldane (1902) who applied this technique to assess the dissolved oxygen and carbon dioxide content of blood. Subsequently, Warburg (1926) measured the oxygen uptake of microorganisms with a manometric apparatus. The apparatus was called a respirometer and functioned by monitoring small pressure changes resulting from biochemical reactions involving gaseous species (Warburg 1926). To our best knowledge, this is the first respirometer in history.

Surprisingly, based on the manometric technique, the oxygen consumption rate of mouse granulosa cells was measured (Hamberger *et al.* 1971). These measurements were made using an elegant technique described earlier by Hamberger *et al.* (1967) for the purposes of investigating the respiratory rate of cells (known as the micro-diver technique). Unfortunately Hamberger *et al.* 1971 did not report any quantitative values for the oxygen consumption rate of the granulosa cells used in the study. Below, the methodology of Hamberger *et al.* (1967) is reviewed as an example of using the manometric technique for measuring the respiratory rate of cells.

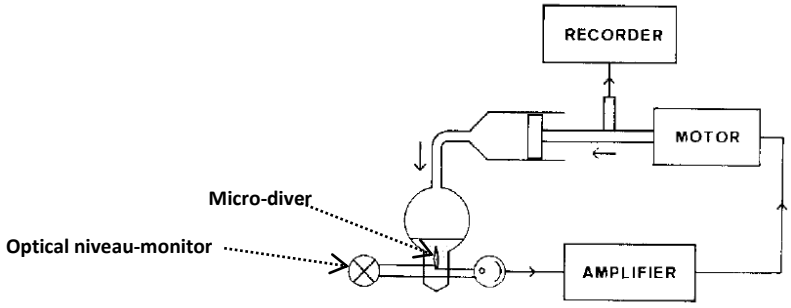

Figure 3.1 Basic structure of the manometric-based measurement system for monitoring the respiratory rate of cells. (Image taken from Hamberger *et al.* 1967).

In this technique, granulosa cells were cultured in the micro-diver. There is an air bubble in the cell suspension, which allows the micro-diver to float in a temperature-controlled buffered solution. As the cells in the diver consume oxygen, the oxygen partial pressure in the air bubble decreases. Thus, the position of the diver tends to descend. In order to keep the diver at same position, the pressure of the closed system needs to be continuously adjusted with the value of the adjusted pressure in each time interval corresponding to the oxygen uptake of the cells.

According to Figure 3.1, an optical “niveau-monitor” is employed to ascertain the level of the micro-diver. The signal from the optical “niveau-monitor” is passed through to a motor which controls the pressure of the closed system to keep the diver at a constant level. The adjusted pressure value is recorded.

In conclusion, this technique allowed the respiratory rate of cells to be quantitatively investigated for the first time. The continuous change of oxygen partial pressure in the cell culture can be directly obtained. Other techniques, such as amperometric and optical technique, require the conversion from the detected electronic or optical signal to the corresponded value of oxygen partial pressure by precise calibration. However, it appears that description of the use of such manometric devices is absent from modern literature, having apparently been replaced by amperometric and optical devices. Unlike amperometric and optical devices, manometric devices appear to be unavailable commercially. Hence, use of a manometric system would require such a device to be built. This would require expertise outside of the scope of this project and likely be very time consuming. For these reasons, the use of a manometric based device was considered unfeasible for this work.

3.2.3 Amperometric technique

The application of the amperometric technique for continuously monitoring dissolved oxygen content is usually carried out by using a Galvanic electrode or a Clark electrode. Thus, the review on amperometric techniques will be conducted based on these two types of electrodes. The principles behind the technique as well as the associated problems will be detailed and discussed.

3.2.3.1 Clark electrode

Figure 3.2 depicts a basic structure of a Clark electrode.

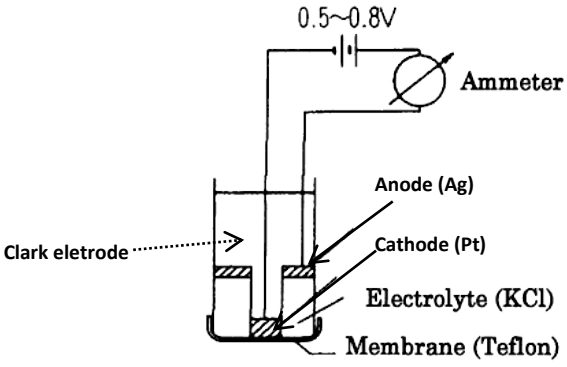

Figure 3.2 Structure of a Clark electrode (Image taken from Global Environment Centre Foundation 1997)

The top of the Clark electrode is sealed by an oxygen permeable, ion-impermeable membrane. The dissolved oxygen in aqueous sample solution can diffuse into the electrode. The membrane also serves the purpose of preventing contamination of the electrolyte (KCl) by solutes in the aqueous sample solution. Such contamination can damage the electrode. The internal electrode is polarised to a 0.5-0.8V potential difference by an external voltage source. Thus, as the dissolved oxygen in the aqueous solution reaches the cathode, reactions are triggered at the both cathode (Pt) and anode (Ag) in the electrolyte (KCl): $O_2+4e^-+2H_2O\rightarrow 4OH^-$ and $4Ag+4Cl^-\rightarrow 4AgCl+4e^-$. Each consumed O_2 molecule at the cathode will result in the transfer of 4 electrons; hence, a current is produced. The dissolved oxygen content is proportional to the current which is measured by the ammeter. Based on the amperometric signal, the corresponding dissolved oxygen content can be obtained by calibrating the electrode in serial known oxygen content medium (Global Environment Centre Foundation 1997; Eutech Instruments Pte Ltd 1997).

The Clark electrode was used by Gosden & Byatt-Smith (1986) to measure the oxygen consumption rate of ovine granulosa cells. Hence, the Clark electrode would appear to be suitable for the purpose of this work. However, according to a report (Eutech Instruments Pte Ltd 1997), there are several problems associated with the Clark electrode, such as isolation of the anode caused by AgCl crystals produced at the anode which coat the surface of the anode over time, pH change and depletion of Cl^- ions in the electrolyte solution. Furthermore, the Clark electrode requires at least 10 min to stabilize before each experimental run. Clark electrodes are also typically large. Though some electrodes cased in a needle are available commercially, the small size dictates that the oxygen permeable membrane is very thin and fragile which can result in the data produced being highly variable should the membrane be inadvertently damaged during measurement.

More importantly, the functionality of Clark electrode results in the continuous consumption of dissolved oxygen in aqueous solution. Thus, the oxygen consumption of the electrode can be significant if the measurement is conducted for a long time or the oxygen consumption rate of the electrode is of comparable magnitude to that of the sample. These issues in combination dictate that the Clark electrode may be inconvenient and not suitably accurate for this work. This is particularly true when one considers the small size of the samples likely to be used in this work.

3.2.3.2 Galvanic electrode

Figure 3.3 depicts structure of a Galvanic electrode.

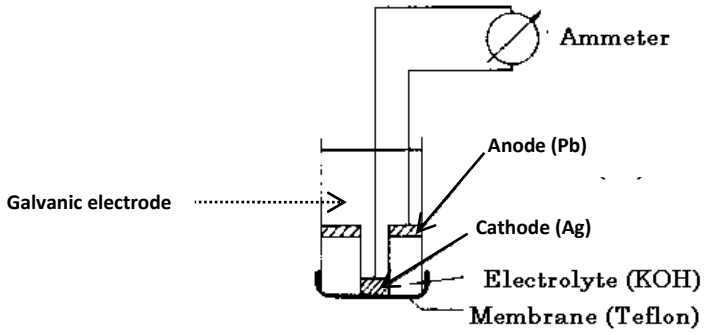

Figure 3.3 The structure of Galvanic electrode (Image taken from Global Environment Centre Foundation 1997).

Unlike the Clark electrode, the idea of Galvanic electrode does not require external polarization. Rather, the potential difference in the electrode for triggering the reactions with the dissolved oxygen from aqueous solution is accomplished by using two dissimilar metals: the noble metal Ag (cathode) and base metal Pb (anode). In the presence of the electrolyte (KOH), an electromotive voltage can be generated between the two metals (Eutech Instruments Pte Ltd 1997).

Compared with the Clark electrode, the Galvanic electrode does not require time to warm up before measurement because the Galvanic electrode is self-polarising and, hence, is always ready for use. The reactions at both cathode (Ag) and anode (Pb) are triggered as the dissolved oxygen reaches the cathode ($O_2+2H_2O+4e^-\rightarrow 4OH^-$ and $Pb+4OH^-\rightarrow PbO_2+2H_2O+2e^-$). Thus, the principle behind the Galvanic electrode for assessing the dissolved oxygen in aqueous solution is similar to Clark electrode, which is based on the current generated by continuously consuming the dissolved oxygen. Moreover, the reactions also suggest that the cathode is gradually corroded by the continuously produced PbO_2. Thus, maintenance of the electrodes is necessary (Eutech Instruments Pte Ltd 1997).

As discussed above for the Clark electrode, this work requires that oxygen depletion in the cell suspension is only caused by cell respiration. The oxygen consumption by amperometric electrodes is potentially problematic for this work and hence the Galvanic electode is considered to be unsuitable for this work also.

3.2.4 Optical techniques

Optical techniques for monitoring dissolved oxygen levels have gained increased popularity in more recent times and are now very commonly used in studies for measuring respiratory rates of cells. Thus, the use of the technique for fulfilling the purpose of this work is promising. After

an initial review of the principles behind this technique, the application of optical techniques to assess/monitor dissolved oxygen content as well as the methodologies for measuring the oxygen consumption rate of granulosa cells are presented below.

3.2.4.1 Background knowledge and theoretical application of optical techniques to assess oxygen levels

As a substance absorbs photons, the energy of the substance increases, which promotes the substance to an excited-state. As the substance emits light, the energy of the substance decreases toward its ground-state. Light which is emitted from the substance is termed luminescence.

Luminescence is classified into two categories, which are fluorescence and phosphorescence. Dissolved oxygen content can be assessed by taking advantage of either of these properties. However, fluorescence based techniques are more common and will be described in more detail here (though the basic principles of phosphorescence based techniques are similar). As an excited fluorophore encounters oxygen, the lifetime and intensity of fluorescence decrease. The fluorescence is said to be quenched by oxygen. According to Stern-Volmer equation (equation 3.1; 3.2), the magnitude of decrease of the lifetime and intensity of the fluorescence is proportional to quantity of the quencher (in this case oxygen). Thus, oxygen can be assessed based on either the quantitative decrease of lifetime or intensity of the fluorescence. The Stern-Volmer equations for fluorescence lifetime (3.1) and intensity (3.2) are,

$$\tau_o/\tau = 1 + K_{sv}Q \quad (3.1)$$

$$I_o/I = 1 + K_{sv}Q \quad (3.2)$$

Where, τ and I represent the lifetime and intensity of fluorescence in the presence of oxygen. τ_o and I_o are the values of lifetime and intensity of the fluorescence in the absence of oxygen. Q represents the dissolved oxygen content. K_{sv} is the Stern-Volmer quenching constant (John *et al.* 2003; Peterson *et al.* 1984).

Based on the above equations the dissolved oxygen content can be determined from a measured intensity or lifetime if the values of K_{sv}, τ_o and I_o are known. The most common way of determining these values is via a simple two point calibration (Slininger *et al.*1989; De Castro e Paula *et al.*2008).

One calibration point is often obtained by measuring the response of the fluorophore in air saturated sample media (0.21 atm). Thus, the measured value of the intensity or lifetime of the fluorescence corresponds to 0.21 atm.

The other calibration point is most often measured in an oxygen-free solution in which oxygen has been removed either by adding a chemical reagent (typically Sodium Sulphite) or sparging with an inert gas (typically nitrogen). Thus, the measured value of the intensity or lifetime of the fluorescence corresponds to 0 atm.

Having obtained these two data points, it is a simple matter to calculate K_{sv} as the slope of a straight line connecting the points (by plotting τ_o/τ vs O_2 (atm) or I_o/I vs O_2 (atm).

3.2.4.2 Practical application of optical techniques

In current studies, optical technique based methodologies for measuring dissolved oxygen content as well as the respiratory rate of cells are based on solid-state oxygen sensors and water-soluble oxygen sensors. Thus, the practical application of optical techniques will be reviewed by considering these two types of sensors.

3.2.4.2.1 Solid-state oxygen sensor

A Solid-state oxygen sensor refers to a luminescent dye (fluorophore or phosphorescent dye) that is immobilized at a single location. In general, the sensor is coated by a microporous membrane which is oxygen permeable, but solution impermeable.

A basic set-up for a solid-state oxygen sensor for monitoring the dissolved oxygen content is depicted by Figure 3.4.

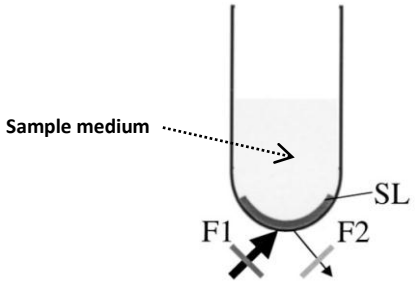

Figure 3.4 Structure of an optical measurement system. Where F1 is a filter and excitation light; F2 is a filter and fluorescence. SL is immobilized fluorophore (Image taken from John *et al.* 2003).

Under the excitation light (F1), the fluorophore (SL) is excited. As the dissolved oxygen quenches the fluorophore (SL), the intensity and lifetime of the fluorescence (F2) decrease and is detected by a fluorescence detector.

Based on this basic methodology, solid state oxygen sensors have been used to construct respirometers for the measurement of cellular oxygen consumption. An example is given by Figure 3.5 (O'Riordan *et al.* 2000).

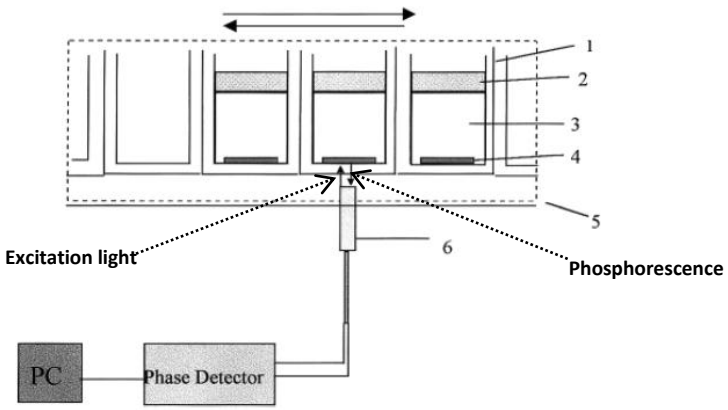

Figure 3.5 Structure of an optical measurement system. Where numbering refers to 1. A strip of the microwell plate; 2. Mineral oil layer; 3. Cell medium; 4. Phosphorescent dye; 5. Thermostated holder; 6. A scanning optical probe, which illuminates the phosphorescent dye and relays phosphorescence to a detector (Image taken from O'Riordan *et al.* 2000).

The cells are cultured in the microwell plate. The cell medium is 'sealed' by the mineral oil layer to prevent air diffusion from the ambient environment. Temperature in the wells is controlled by the thermostated holder. The dissolved oxygen content is sensed by the phosphorescent dye which is immobilized at the bottom of each microwell by a microporous membrane. The phosphorescent dye is illuminated by the optical probe which periodically scans underneath each of the plates. Simultaneously, the phosphorescent signal is transmitted from the optical probe to the detector.

Although the configuration shown in Figure 3.5 is relatively common in the literature, it should be noted that the oil layer will be permeable to oxygen which may make this system somewhat error prone (it is essentially leaking). The magnitude of the error will depend on the degree to which the oil is oxygen permeable. Furthermore, systems such as that depicted in Figure 3.5 often incorporate no mixing and hence may be further error prone due to diffusion gradients existing within the well.

Solid state oxygen sensors may also be arranged so that they are portable and can be placed directly into a sample at the point of interest. Such an arrangement is shown in Figure 3.6 which depicts a portable fluorescence based oxygen sensor.

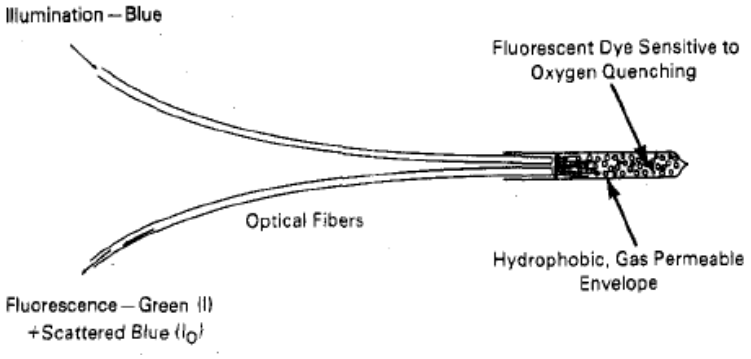

Figure 3.6 A configuration of fiber optic fluorescent probe (Image taken from Peterson *et al.* 1984).

In this configuration, one optical fibre transmits light to illuminate the fluorophore which is packed by a liquid impermeable but highly gas permeable envelope at the tip of the probe. The fluorescence is transmitted to a fluorescence detector by another optical fiber (Peterson *et al.* 1984).

When the tip of the probe is immersed in the sample medium the dissolved oxygen diffuses into the envelope, and the fluorophore is quenched. This results in a change in the intensity and the lifetime of the fluorescence which is received by the detector.

In conclusion, the use of immobilized oxygen sensor for the purpose of this work is limited by the measurement system (Figure 3.5). As discussed above, such respirometers (Figure 3.5) have some disadvantages which contradict the requirements of this work (such as the dubious oil seal). In contrast, the portable oxygen sensor (the optical probe depicted by Figure 3.6) is independent. The optical probe can be repetitively used in different types of oxygen measurement systems by directly placing the oxygen sensor at the point of interest, which makes it more versatile and flexible for a variety of applications. Thus, the probe-format solid oxygen sensor may be more easily incorporated into a respirometer which will be specifically designed for measuring the oxygen consumption rate of granulosa cells.

It is noteworthy that some luminescent dyes are water-insoluble but oil-soluble. Based on this property, oil is used to immobilize the dye in sample medium instead of a microporous membrane. This technique has been applied to measure the oxygen uptake rate of granulosa complexes in which the oocyte in the cumulus-oocyte complex has been microsurgically removed by aspiration (Sutton *et al.* 2003). Such granulosa cells are known as cumulus cells and are known to have different functionality to the bulk granulosa cells which are the primary interest of this work.

3.2.4.2.2 Water-soluble oxygen sensor

In these sensors the luminescent dye is not immobilised but rather dissolved and evenly distributed throughout the sample medium. Water-soluble oxygen sensors are most commonly used in conjunction with a phosphorescent dye. In general, water-soluble oxygen sensor-based respirometers are similar to the respirometer depicted by Figure 3.5. The difference is that the water-soluble oxygen dye in respirometer is not immobilized at bottom of each microwell. Instead, the dye is dissolved in the sample medium. The excitation light and the phosphorescence signal detection are, once again, carried out via a plate reader equipped underneath the microwell plate (Castellano & Lakowicz 1998; Alderman *et al.* 2004; Hynes *et al.* 2003).

Water soluble oxygen sensing based respirometers appear to be very precise. For example, such a system was shown to be capable of measuring the respiratory rate of a mere 300 mammalian cells in 3µl of medium. As a result of this precision, this type of sensing has been used to measure the oxygen consumption rate of a wide variety of cells (Alderman *et al.* 2004).

It is noteworthy that lifetime of phosphorescence is independent of concentration of the dissolved phosphorescent dye in medium; instead, they are determined by the quantity of dissolved oxygen (Castellano & Lakowicz 1998). The same authors also proposed that the sensor could be applied to image intracellular oxygen content.

Despite the advantages of water soluble oxygen sensors, they are often associated with cumbersome handling and inaccuracies associated with difficulties in dye dispersion. Furthermore, the effect of the dye on the cell health is unknown. Thus, the use of the water soluble oxygen sensors should be approached with caution.

3.2.5 Conclusion and discussion

In the review above, knowledge regarding existing techniques for assessing dissolved oxygen content and methodologies for measuring cellular oxygen consumption rate were presented. At the same time, the advantages and disadvantages of applying these techniques for the measuring oxygen consumption rate of granulosa cells was discussed.

Based on this review the most suitable measurement device for use in this work is the solid state optical sensor in the format of a probe (Figure 3.6). Based on this selection and the required culture conditions of this work, the next section will consider the design and construction of a suitable respirometer.

3.3 Optical-based preliminary respirometer

In some studies, the measurement of cellular oxygen consumption rate in cell suspensions was accomplished by amperometric-based respirometers in which the cells were cultured in specific conditions and the dissolved oxygen in the cell suspension was monitored by either a Clark or Galvanic electrode. Except for the inherent oxygen consumption by the electrode, the previous methodologies are basically suitable for measuring the oxygen consumption rate of granulosa cells; thus, it is worthwhile examining the methodologies associated these amperometric-based respirometers first.

3.3.1 Review on amperometric-based respirometers

Both the Clark and Galvanic electrodes have been used to construct respirometers for various applications in the literature, including measurement of cellular respiration. Figure 3.7 depicts an example of one such respirometer (left) and its modified Clark electrode (right) (Rank Brothers Ltd 2002; University of Leeds 2010).

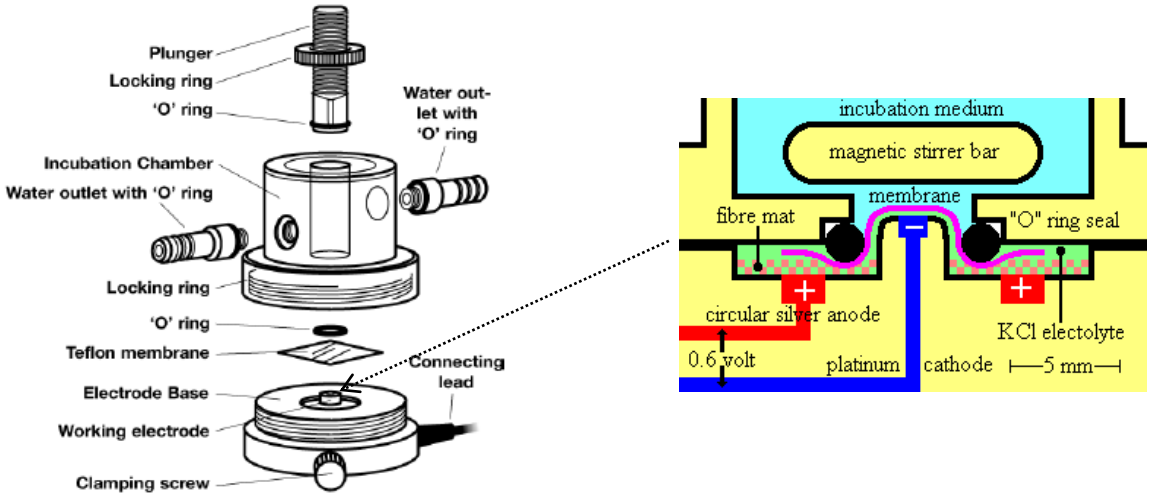

(Rank Brothers Ltd 2002) (University of Leeds 2010)

Figure 3.7 Structure of a respirometer (left) and its modified Clark electrode (right) (Images taken from Rank Brothers Ltd 2002; University of Leeds 2010)

Cells are suspended by the culture medium in the incubation chamber (Figure 3.7 left); a modified Clark electrode (Figure 3.7 right) is fixed at bottom of the incubation chamber to monitor dissolved oxygen change in the cell suspension. The structure of the respirometer is such that the incubation chamber is air tight and temperature-controlled (Figure 3.7 left). Furthermore, a magnetically-coupled stirrer bar is placed at the bottom to eliminate any oxygen concentration gradient in the cell suspension and help ensure the cells are evenly dispersed.

Figure 3.8 depicts another example of respirometer incorporating a Clark electrode.

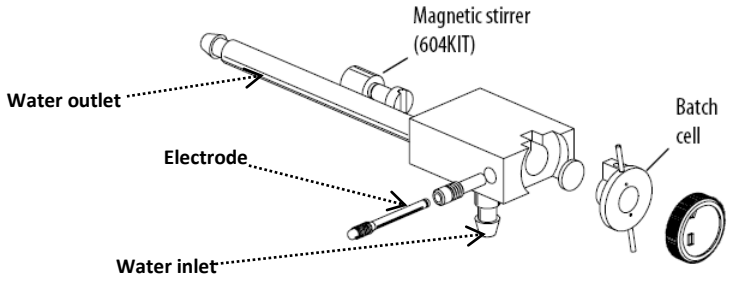

Figure 3.8 Structure of a respirometer (Image taken from Instech Laboratories 2009)

This respirometer not only possesses the functionality of the previous examples (depicted by Figure 3.7) but also has a tiny incubation chamber which is only 600µl. This allows measurement of respiratory rate of small quantities of cells (Instech Laboratories 2009).

In section 3.1, this work proposed specific culture conditions required for the measurement. According to the functionalities of the respirometers exhibited by Figure 3.7 and 3.8, the proposed conditions could be achieved in both of the respirometers. The functionalities are fulfilled by,

(i) The locking rings and O-rings which seal the incubation chamber to prevent air leakage.
(ii) A magnetically-coupled stirrer bar for mixing the medium so that oxygen gradient can be eliminated and even cell suspension maintained.
(iii) Circulated water around the chamber for temperature control.
(iv) An oxygen sensor (in this case, an amperometric electrode) which can continuously monitor the dissolved oxygen content.

These four components above are important for the respirometers to fulfil the functionality of measuring the oxygen consumption rate of cells suspended in culture medium. These four components will be embodied in the new respirometer which is particularly designed to measure the oxygen consumption rate of granulosa cells. Furthermore, to overcome the drawback of amperometric electrodes (they consume oxygen), this work will use an optical probe instead of an amperometric electrode to monitor the dissolved oxygen content. The design of such a respirometer will be described in the next section.

3.3.2 Design of the preliminary respirometer

As a starting point for respirometer design, the scale of the respirometer needs to be evaluated based on the quantity of harvested granulosa cells. Moreover, the material for constructing the respirometer also needs to be considered. Any such material (s) should be readily available, easy to be work with and most importantly, impermeable to oxygen.

According to the preliminary collection and processing of granulosa cells, which will be described in Chapter 5, the maximum practical sample volume (cells plus media) which can be

reasonably collected in a single visit to the abattoir is approximately 2 ml, which is consistent with the volume used in previous granulosa based measurement (Gosden & Byatt-Smith 1986).

Steel will be used as a construction material for the initial respirometer. Steel is readily available, relatively easy to work with and is impermeable to oxygen.

Based on the components listed in the last section, the initial design of the respirometer is as follows will incorporate the following,

Firstly, the granulosa cells are cultured in 2 ml vertical chamber. The opening of the chamber is sealed by a screw cap. An optical probe is introduced into the chamber from the top of the cap and the tip protrudes out of the bottom. Thus, the dissolved oxygen content will be monitored at top of the chamber. At the bottom of the chamber, a magnetically-coupled stirrer is placed to mix the culture medium, which will facilitate even suspension of granulosa cells, and also eliminate any oxygen gradients. In order to sustain 37°C during measurement, the respirometer will be submerged in water bath.

3.3.3 Preliminary respirometer design and build

Based on the concepts described above, a respirometer was manufactured. The basic components of the respirometer (an incubation chamber, a screw cap and a base) are displayed in Figure 3.9 and 3.10. The assembled respirometer is shown in Figure 3.11. Detailed information regarding the optical probe will be given in the next section.

Figure 3.9 shows the incubation chamber and stirrer.

Figure 3.9 A 2 ml incubation chamber (the internal diameter is 8mm; 40mm deep) shown from different perspectives. Where the thread, the O-ring and the stirrer (3.3mm in diameter, manufactured by Sigma-Aldrich Co. LLC., Missouri, USA, product no. z283835) are indicated by arrowheads.

Figure 3.10 shows the screw cap of the incubation chamber and the introduced optical probe.

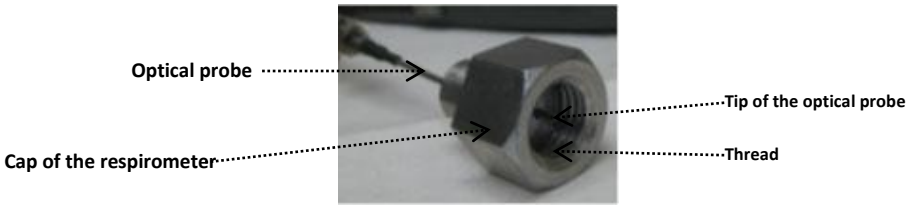

Figure 3.10 The screw cap of the incubation chamber. Where the tip of the optical probe, the thread and the optical probe are indicated by arrowheads.

The optical probe is completely fixed to the cap by adhesive (super glue). The tip of the optical sensor protrudes 2mm out of the bottom of the cap, where the dissolved oxygen in the cell suspension will be sensed (Figure 3.10). There is a thread in the internal wall of the cap, which matches the thread on the external wall of the incubation chamber so that the chamber can be closed by screwing the incubation chamber into the cap (Figure 3.11 left). The bottom of the chamber is screwed into a base so that the chamber can be enclosed and sealed by tightly screwing the cap and the base against the O-ring which is located between the cap and the base to prevent the diffusion of air into the incubation chamber from the ambient environment (Figure 3.11 right).

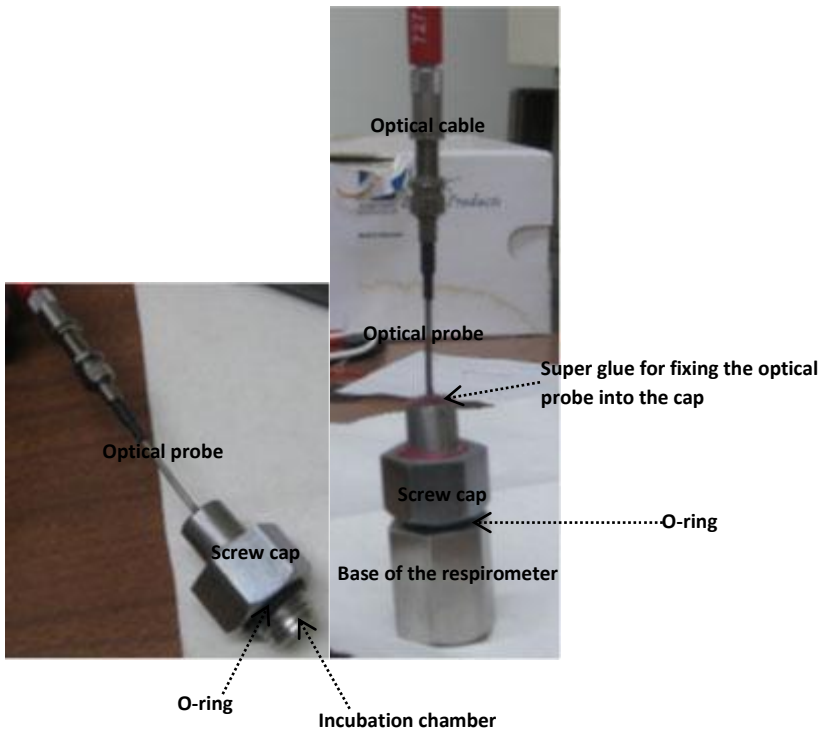

Figure 3.11 The chamber is screwed into the cap (left). The whole respirometer (right).

Unlike the respirometers displayed by Figure 3.7, the proposed respirometer (Figure 3.11 right) does not include a water circulation system. Instead, it will be used in a temperature-controlled water bath. A magnetic stage is placed underneath the water bath to drive the magnetic stirrer to achieve the proposed culture conditions.

3.3.4 The optical device

The commercially available optical sensing system used in this work is the NeoFox (Ocean Optics Inc., California, USA) which is depicted by Figure 3.12.

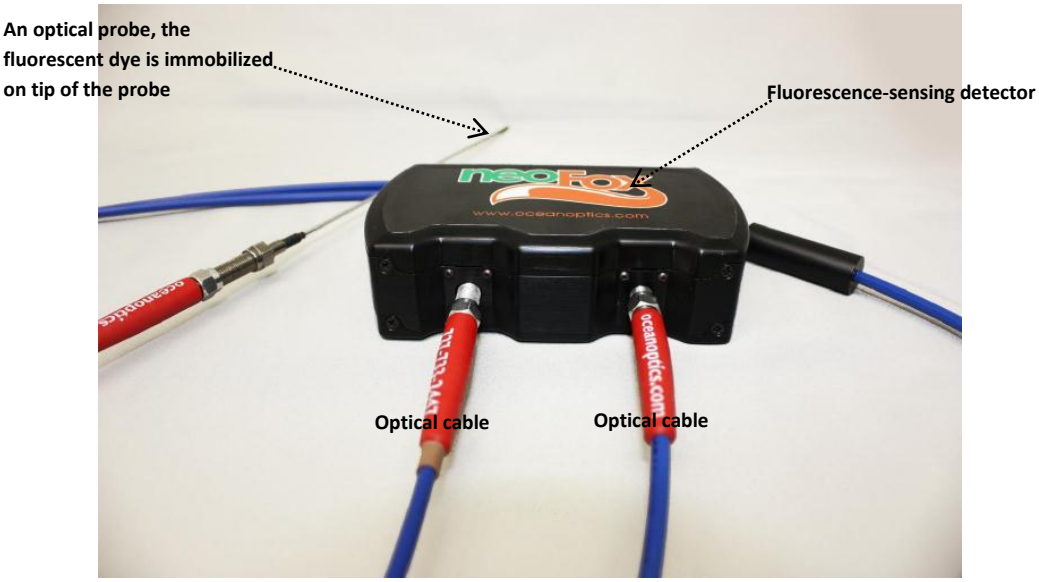

Figure 3.12 The NeoFox which basically consists of four accessories. Where each accessory is indicated.

The configuration of the optical probe in Figure 3.12 is similar to the probe depicted in Figure 3.6. One optical cable delivers the LED excitation to illuminate the fluorescent dye at the tip of the probe. Another transmits fluorescence from the tip to the fluorescence-sensing detector which monitors the real-time change in life time of the fluorescence caused by oxygen quenching. Values of the life time of fluorescence are transmitted to a computer via a USB cable. Calibration of the optical probe is conducted using two points of known oxygen content in granulosa cell culture medium (see section 3.4), in which the two points, 0.21 atm and 0 atm in this work, are achieved by sparging air and nitrogen into the medium respectively (further details of the two point calibration are described in detail in section 3.2.4.1). After the two point calibration, competency of the probe response to the oxygen partial pressure changes in the culture medium was tested by sparging gases which contain different oxygen partial pressure into the medium (Figure 3.13).

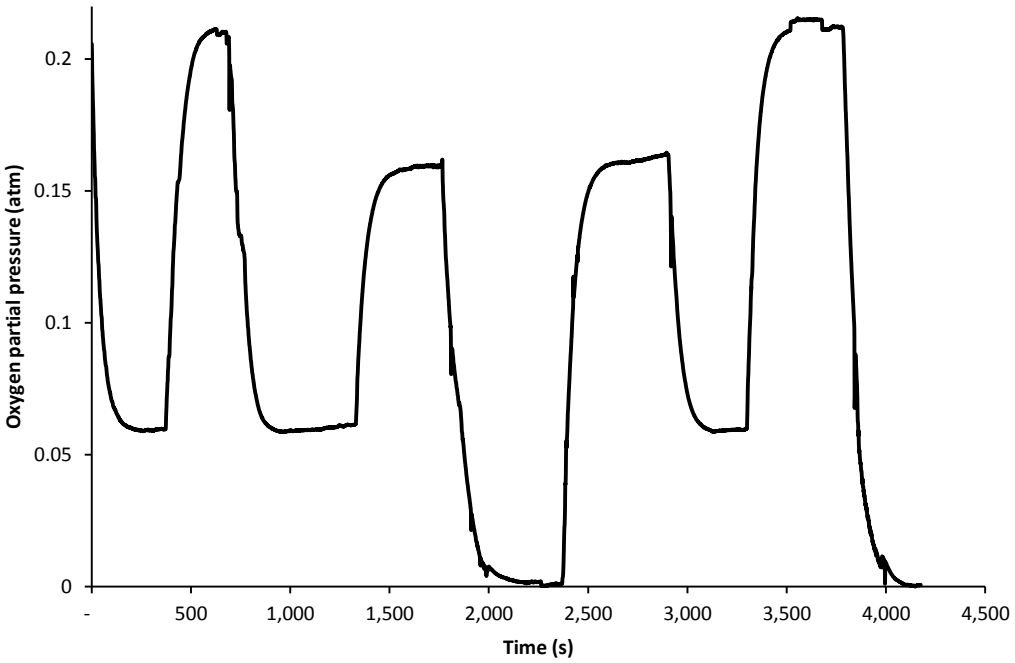

Figure 3.13 The response of the optical probe to the changes of the oxygen partial pressure in the granulosa cell culture medium at 37°C. Step changes to various oxygen levels are depicted (0.06, 0.16, 0.21 and 0 atm).

As shown in Figure 3.13, the optical probe responds well to changing oxygen levels in the culture medium. This suggests that the optical device should be able to continuously monitor the real-time change of oxygen partial pressure in the granulosa cell suspension.

In the next section the proposed respirometer will be tested with actual granulosa cells.

3.4 Resiprometer testing

Before the respirometer was tested granulosa cells were collected from a local abbotoir. A detailed description of the initial methodology used to collect and process these cells can be found in section 5.1.

Based on expert advice from those experienced in granulose cell culture this work used Dulbecco's Modified Eagle Medium (DMEM) (Life Technologies Corporation, Auckland, New Zealand, product no. 11995065) to culture granulosa cells.

To start the measurement, the optical probe, attached with its cap, was calibrated in DMEM at 37°C, and then the incubation chamber was filled by the cell suspension (granulosa cells suspended in culture medium) was enclosed by screwing the cap and the base against each other. The measurement of oxygen consumption rate of the granulosa cells started as the respirometer was placed into a water bath at 37°C, and the magnetic stage turned on. In this measurement, two stirrers were placed in the chamber to mix the cell suspension.

Figure 3.14 depicts the oxygen partial pressure profile of data collected during measurement of granulosa cell oxygen consumption in the respirometer.

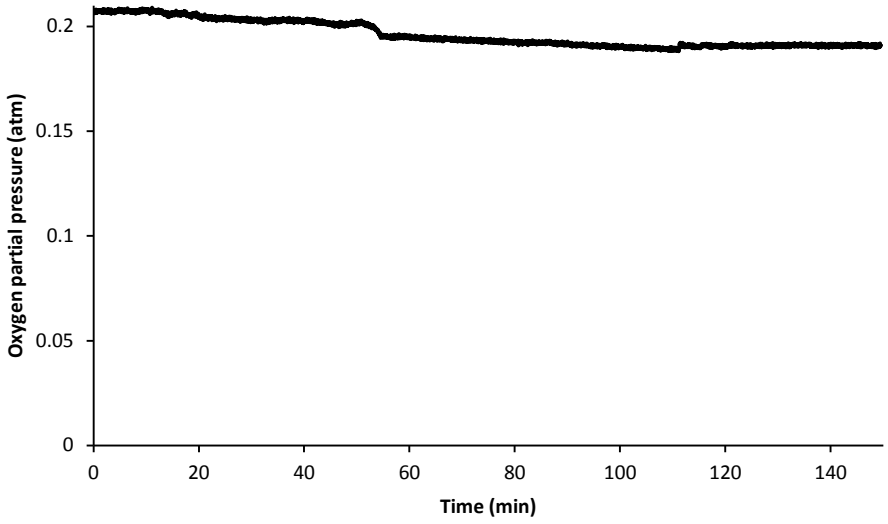

Figure 3.14 Oxygen partial pressure (atm) in the granulosa cell suspension as a function of time during the measurement

Figure 3.14 shows that the oxygen partial pressure in the granulosa cell suspension decreases by only 0.018 atm over approximately 109 min. Moreover, the oxygen partial pressure rose up at end of the measurement. This potentially represents a failure to accurately determine the oxygen consumption rate of the granulosa cells. Potential causes of this apparent failure are examined in the next section.

3.5 Problems with the measurement

Successful measurement of the oxygen consumption rate of granulosa cells required that a significant decrease in the oxygen content of the respirometer be observed over the time course of measurement. The previous section showed that this was not the case. Since this work has demonstrated the competency of the optical probe (Figure 3.13), the most likely causes of this failure are,

(i) Cell death – cell death during measurement would result in lower and less rapid observed decline in respirometer oxygen content than would be expected.
(ii) Leaking – respirometer leaking would result in the same effect as cell death with the additional possibility that the oxygen content of the respirometer may increase (since it is surrounded by ambient air).
(iii) Air voids – this work has not confirmed that the chamber filled by cell suspension can completely fill the space under the cap after the respirometer is assembled. The presence of the air voids would provide oxygen to the cell

suspension; thus, the oxygen depletion caused by cell respiration during the measurement cannot be accurately measured.

These issues are considered in the following sections.

3.5.1 The granulosa cells in the respirometer

After the measurement described in Figure 3.14, the granulosa cell suspension with two stirrers was poured into a petri dish for observation (Figure 3.15).

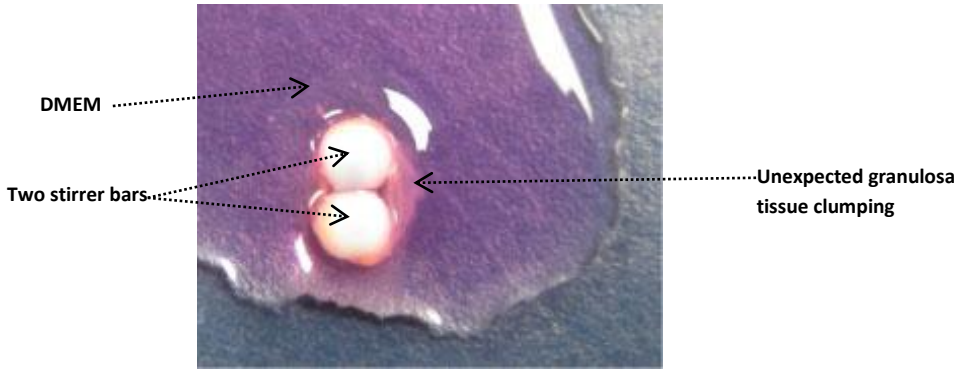

Figure 3.15 Respirometer contents after measurement. Where two stirrers, unexpected granulosa tissue clumping and DMEM are indicated by arrowheads.

Visible in Figure 3.15 is unexpected granulose tissue clumping. This indicates that the desired dispersed/suspended state of the granulosa suspension was not achieved. Figure 3.16 shows this tissue after isolation from the stirrers.

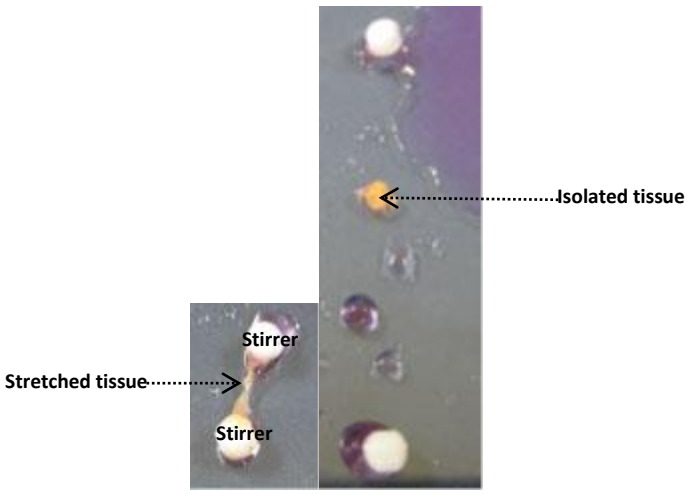

Figure 3.16 The tissue is stretched (left) and isolated (right). Where, the two stirrers and tissue are indicated.

The tissue was adhesive and elastic. The tissue assumed the shape of a spherical clump (mass~1mg) after it was isolated from the stirrers.

To assess the cell viability, the tissue was stained by Trypan blue solution in which dyed cells were stained blue (see Section 2.5.4.2) when observed under a microscope (Figure 3.17).

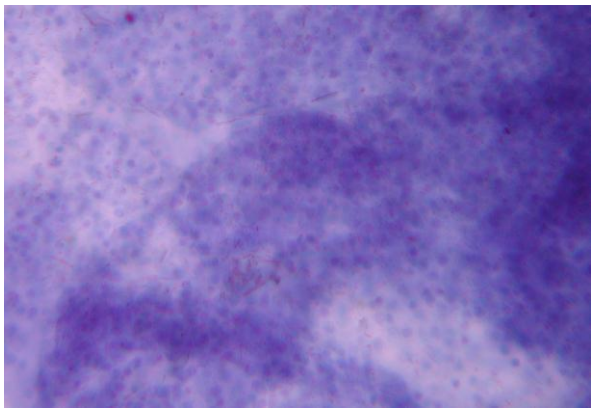

Figure 3.17 Image of the tissue at 400 × magnification.

According to Figure 3.17, the tissue is composed almost entirely of the stained granulosa cells, indicating an overwhelming absence of viable cells.

It is likely that the failure to achieve the desired cell suspension has caused the observed cell death. The observed cell clumping likely results in diffusion limitations which cause all but the outermost granulosa cells to be starved of essential nutrients in the culture media (most crucially, oxygen). In addition, the observed clumping makes cell counting practically impossible.

Furthermore, the DMEM media was observed to change colour between the start and end of the experimental run. This indicates a pH change in the media and is likely result of the absence of a pH buffer in the DMEM. Cell respiration during the measurement may cause these pH changes which could affect the cell viability. Thus, this type of DMEM may be not suitable for culturing cells in the isolated condition; a new culture medium is required.

The problems described above will need to be resolved to enable the successful measurement of granulosa cell oxygen consumption rate. These issues will be addressed in subsequent chapters.

3.5.2 Respirometer oxygen profiles

Because of the observed problems with cell death etc. it is not possible to tell if the respirometer is functioning correctly with regard to oxygen measurement. The problems in the respirometer may be due to leaking or air voids (see Section 3.5). Either of these issues could result in the observed rise in oxygen partial pressure. This section aims to investigate if these problems are present in the respirometer.

The possibility of air voids was examined first according to the methodology described below.

Nitrogen was sparged into the sample medium (DMEM) to reduce the dissolved oxygen content. The sample was then immediately loaded into the chamber until it was filled. The respirometer was rapidly assembled, and then immersed into a nitrogen saturated water bath at 37°C, in which the water was continuously sparged with nitrogen. The oxygen partial pressure was then monitored over time and is shown in Figure 3.18.

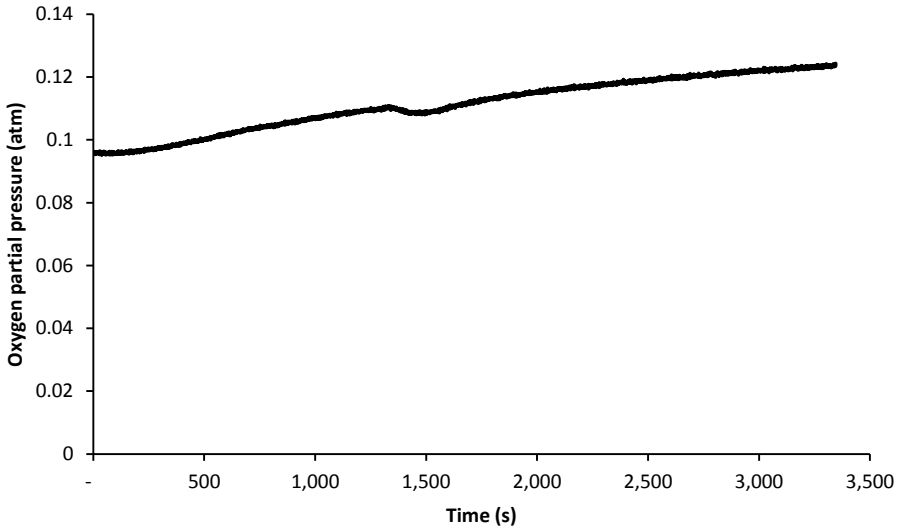

Figure 3.18 Oxygen partial pressure change over time in the respirometer

Figure 3.18 shows that the initial oxygen partial pressure in the respirometer is 0.096 atm. The low oxygen partial pressure is due to the initial nitrogen sparing. From this initial level the oxygen partial pressure gradually increases to 0.12 atm over 55 minutes.

This measurement was conducted in the nitrogen saturated water to eliminate the possibility of oxygen entering the respiration chamber from ambient air. Thus, the increase in the oxygen partial pressure in the DMEM reveals that there must be an internal oxygen source in the respirometer. Hence, air voids must be present in the respirometer. This is likely due to the fact that the medium cannot completely occupy the space under the cap after the respirometer is assembled. This unexpected defect relates to the structure of the respirometer.

Essentially this means that the design of the respirometer must be reconsidered to eliminate the presence of air voids. As a result, the examination of the possibility of air leakage in the current design is no longer relevant.

3.6 Conclusion

Based on a review of existing techniques, this work selected an optical device to monitor dissolved oxygen content in the granulosa cell suspension. The competency of the optical device has been verified by the experimental work described (Figure 3.13).

However, the measurement of oxygen consumption rate of the granulosa cells was unsuccessful. This was the result of a number of issues which were identified. Firstly, massive cell death was observed after the measurement; and is likely caused by granulosa clump formation and the pH change in the DMEM culture medium. Flaws in the structure/design of the respirometer were also identified as resulting in the presence of air voids in the incubation chamber, rendering it incapable of reliable measurement.

These problems are unacceptable because they result in failure to achieve the respirometer specifications required for this work. To ensure the viability of granulosa cells during the measurement, methodologies for cell dissociation and prevention of clump formation need to be developed. Also essential is a competency of the respirometer in terms of oxygen measurement reliability. The air voids in the preliminary respirometer may be eliminated or circumvented by modification to the respirometer design.

Hence, the re-design, construction and testing of a new respirometer are the subject of the next chapter. Issues surrounding cell culture conditions will be addressed later in this work.

Chapter 4. A new respirometer

Previously, use of the proposed respirometer was shown to be handicapped by the presence of air voids. To inspire the design of a new respirometer, this chapter will start by reviewing an existing respirometer, in which an optical probe (identical to that used in this work) is applied to monitor the change of oxygen content in a sample chamber. A respirometer will then be designed by readdressing the basic required functionalities of the measurement system (see Section 3.3.1) and the issue of the presence of air voids. A new respirometer will be constructed; its competency tested to determine the success of the redesigned system.

4.1 Review of an existing respirometer (developed by Brown 2011)

One of the requirements of the respirometer is that the connection between the optical probe and respirometer must be air tight and stable. Previously, this requirement was achieved by using glue to fix the tip of the optical probe to the cap of the respirometer (Figure 3.11). This has a major disadvantage that the probe cannot be removed from the system. This is undesirable largely due to the expense of the optical probe which essentially becomes locked into the system, making it somewhat useless for other purposes and difficult to replace should it become faulty.

A respirometer which overcomes this difficulty is that described by Brown (2011, personal communication). This respirometer is depicted in Figure 4.1. The device was designed to measure the rate of oxygen consumption during the oxidation at oils. Even though the purpose is different from measuring cellular respiration, this device presents a method to connect the optical probe with the respirometer whilst still allowing it to be detached from the system. More importantly, the device was designed to overcome the issue of air void.

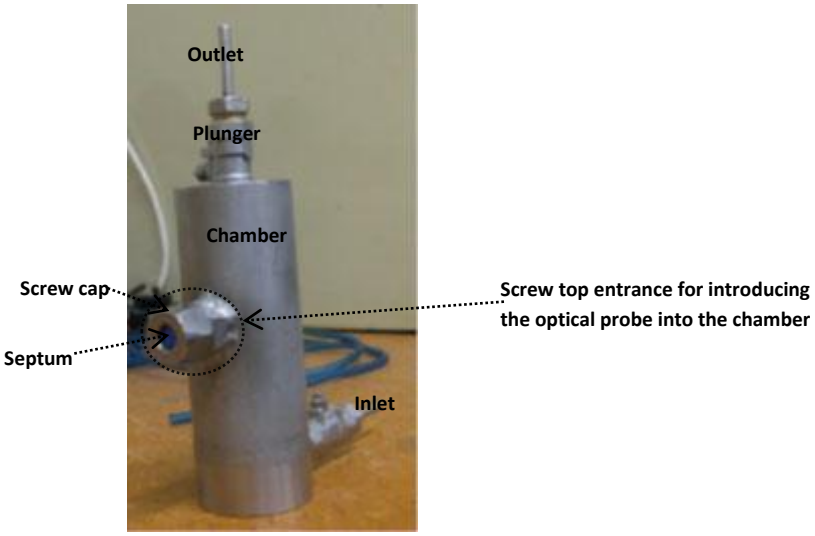

Figure 4.1 Image of the 120 ml respirometer (Brown 2011) showing the screw cap, screw top entrance, outlet, plunger, chamber, inlet and septum (made of Teflon).

In this respirometer, the optical probe is inserted into the 120 ml sample chamber prior to measurement and can be withdrawn at the end of an experimental run. This is achieved by inserting and/or withdrawing the probe through a replaceable septum (made of Teflon) located at the side of the chamber. Experimental testing of this respirometer has demonstrated that the system is air tight and the connection between the optical probe and respirometer is stable.

Besides the withdrawable probe, this respirometer exhibits other merits. The respirometer can remove any extra gas out of the chamber. In light of the problem caused by air voids in the preliminary respirometer, the functionality of extra gas removal is desirable. Furthermore, the optical probe can be calibrated in place after insertion into the sample chamber which eliminates any issues associated with the possible change in probe response if it is calibrated in a separate location to where measurement is made. Operation of this respirometer to achieve these functionalities is described below.

The first step is probe calibration.

(i) The respirometer is opened by pulling the plunger out of the chamber, and then loading the calibration medium in.
(ii) The chamber is closed by reinserting the plunger, and then pushing the plunger along the chamber until some medium comes out of top of the plunger (the outlet). This ensures any remaining gas is removed from the sample chamber.
(iii) The optical probe is introduced into the chamber via the septum, and calibration gases are passed through the chamber via the inlet and exit through the outlet. The inlet and outlet are controlled by two valves (not visible in Figure 4.1).

After calibration, measurement is conducted.

(i) The calibration medium is withdrawn from the inlet.
(ii) The plunger is pulled out and the sample medium is placed into the chamber.
(iii) Once again, the plunger is reinserted and the extra gases are removed by applying pressure to the plunger until a small amount of sample media overflows from the outlet.
(iv) After closing the inlet and outlet, the measurement of dissolved oxygen content in the sample starts.

The calibration and measurement are typically carried out in an incubator or submerged in a water bath to facilitate temperature control.

The main difficulty in applying the described respirometer to the measurement of oxygen consumption of granulosa cells is in the large size of this respirometer. This work is limited by the amount of granulosa cells that can be collected. Thus, the size of the described 120 ml system needs to be reduced. This may make some of the functionalities of the 120ml respirometer, such as extra gas removal and optical probe calibration challenging to implement in a smaller system.

However, the functionality for inserting/withdrawing the optical probe, which is exhibited in the larger system, can easily be retained on a smaller scale. This could be achieved simply by creating a respirometer of a small fixed volume with a screw seal septum seal similar to that shown in Figure 4.1. This would retain the desirable feature of the probe being removable. Such a system will be described in the next section along with ways to avoid the presence of air voids in the small system.

4.2 A new respirometer proposal

The basic concept of the new respirometer was to encapsulate a small volume of cell suspension around tip of the optical probe where the dissolved oxygen in the cell suspension can be monitored. This is achieved by placing the cell suspension in a chamber with a septum seal which allows the optical probe can be inserted and removed from the chamber.

The basic structure of chamber of the new respirometer can be embodied by Figure 4.2.

Figure 4.2 Basic structure of the chamber of the new respirometer depicted by the image of the optical probe entrance at the respirometer of Brown 2011. Where each proposed accessory of the chamber is indicated by arrowhead.

Figure 4.2 depicts the chamber which consists of a screw cap, a screw top opening and a septum. The chamber is sealed with a septum located underneath the screw. The screw top is turned until a tight seal is created between the septum and the entrance to the chamber. The central part of the septum is exposed so that the optical probe can be inserted into the chamber by penetrating the septum (and subsequently removed as designed).

This proposed respirometer design does not include an explicit means for removing any air voids which may be present. However, the new respirometer chamber can be constructed of a transparent material such as glass, which will allow any air voids to be easily visualised and subsequently removed. Choosing glass would still allow the respirometer to be air tight since glass is impermeable to air.

The optical probe can be calibrated in place by sparging the sample chamber either with the lid slightly ajar or via small inlet and outlet tubes punctured through the septum. However, it is practically much easier to calibrate the probe in a larger vial prior to insertion into the chamber. This method was problematic in the previous respirometer since the optical probe was encased in a heavy steel forged cap. This resulted in unnecessary strain being placed on the shaft of the probe during transport between the calibration location and the respirometer location. This sometimes resulted in visual disturbance to the probe response. However, this problem can be eliminated by the use of a septum seal which allows the probe can be easily

inserted and removed. Therefore, the probe can be transported without a large mass of steel glued to it.

In summary, the defects exhibited by the previous respirometer can be solved by constructing the respirometer with transparent and lighter material and using a spetum seal for introducing the optical probe. These features will be embodied in the new respirometer.

4.3 Gas chromatography sampling (GCMS) vials

Figure 4.3 exhibits several GCMS sampling vials which were potentially suitable for using as the chamber of the new respirometer.

Figure 4.3 Standard clear vials (2ml)

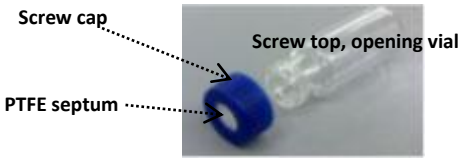

Figure 4.4 A standard 2ml clear glass vial. Where the accessories of the vial are indicated.

The glass vial (Figure 4.4) (Phenomenex Inc., California, USA, product no. AR0-9921-13-C) embodies the proposed structure of the chamber, and also the new features required in the new respirometer (see section 4.2). Furthermore, the 2ml volume just matches the upper end of the practical volume of cell collection. The optical probe can be introduced by penetrating the PTFE (Polytetrafluoroethylene) septum attached underneath of the screw cap (made of polypropylene). Another merit is that the vials are inexpensive and can therefore be disposed of after use.

4.4 The new respirometer

The new respirometer is shown in Figure 4.5 (right), alongside the previous preliminary respirometer (Figure 4.5 left).

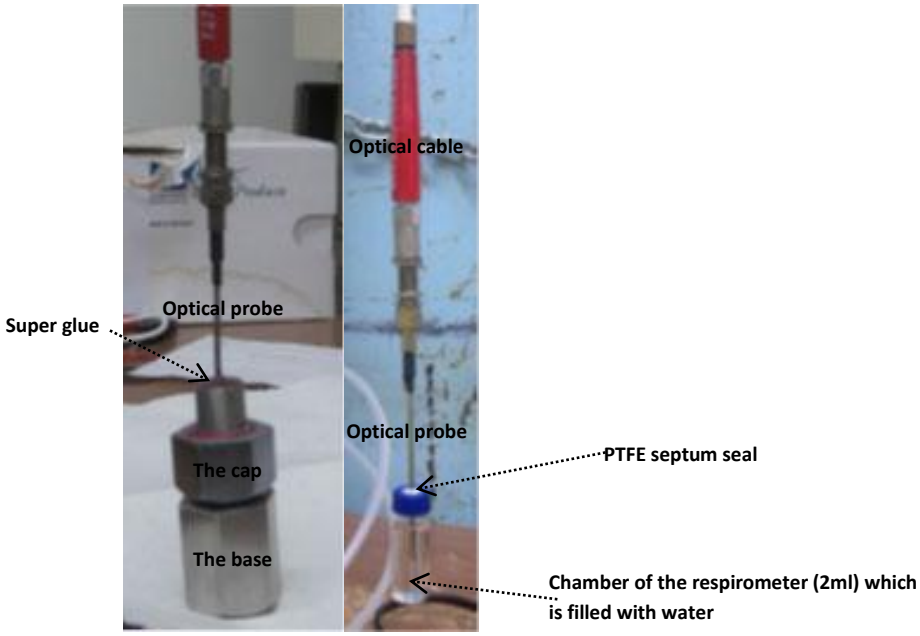

Figure 4.5 The new respirometer (right) and previous preliminary respirometer (left). Where the accessories of the new respirometer as well as the preliminary respirometer are indicated.

The PTFE septum is hard and can potentially damage the probe. To insert the optical probe, the centre of the PTFE septum must be penetrated first with a needle. To eliminate the presence of air voids, the chamber must be filled until the sample forms a bulge at the opening of the chamber. As the cap is screwed on, the extra sample flows out through the punctured hole. The outflow suggests that the space under the cap is completely by sample media. Any remaining gas under the cap should have been forced out of the chamber with the outflow. At this point, the optical probe is inserted through the punctured hole, and the assembly of the new respirometer is complete (Figure 4.5 right).

The major improvements exhibited by the new respirometer are as follows,

(i) The new respirometer has a light chamber (2.35g). This has eliminated any significant observable strain on the shaft of the probe.

(ii) The new respirometer is constructed of transparent glass. This is both impermeable to oxygen and also allows the presence any air voids to be observed with the naked eye (this is particularly obvious if the chamber is inverted as in Figure 4.6).

(iii) The optical probe can be easily inserted and removed. This advantage is associated with the septum. Therefore, the probe can be transported without the previous large mass of steel glued to it and potentially calibrated in place.

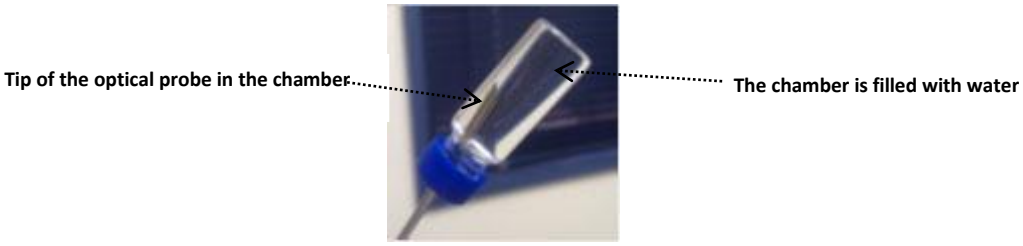

Figure 4.6 The chamber (filled with water and inverted in order to see if any undesirable air bubbles were trapped in the chamber) and optical probe of the new respirometer.

Occasionally, air voids are observed after the respirometer is assembled; in this case, the chamber is opened and reloaded with a small amount of sample to reform the bulge, and then resealed.

Even though it is possible to eliminate air voids in the new respirometer, it still needs to be determined if the new respirometer is impermeable to oxygen. It is possible that gas can enter or leave the respirometer through the cap or septum, especially where the probe punctures the septum. In order to determine if this is an issue, air tight testing was carried out as descried in the next section.

4.5 Air tight testing of the new respirometer

Air tight testing was conducted according to the methodology described below.

Nitrogen was sparged into the sample (water) until the sample was saturated by nitrogen (zero oxygen content), which was detected by the optical probe. This sample was then immediately inserted into the sample chamber and the respirometer was assembled and submerged in a water bath controlled at 22±1°C. The oxygen partial pressure in the sample was monitored over time. In order to justify the results of testing, 5 replicate measurements were conducted.

The two representative results of the measurements are shown by Figure 4.7.

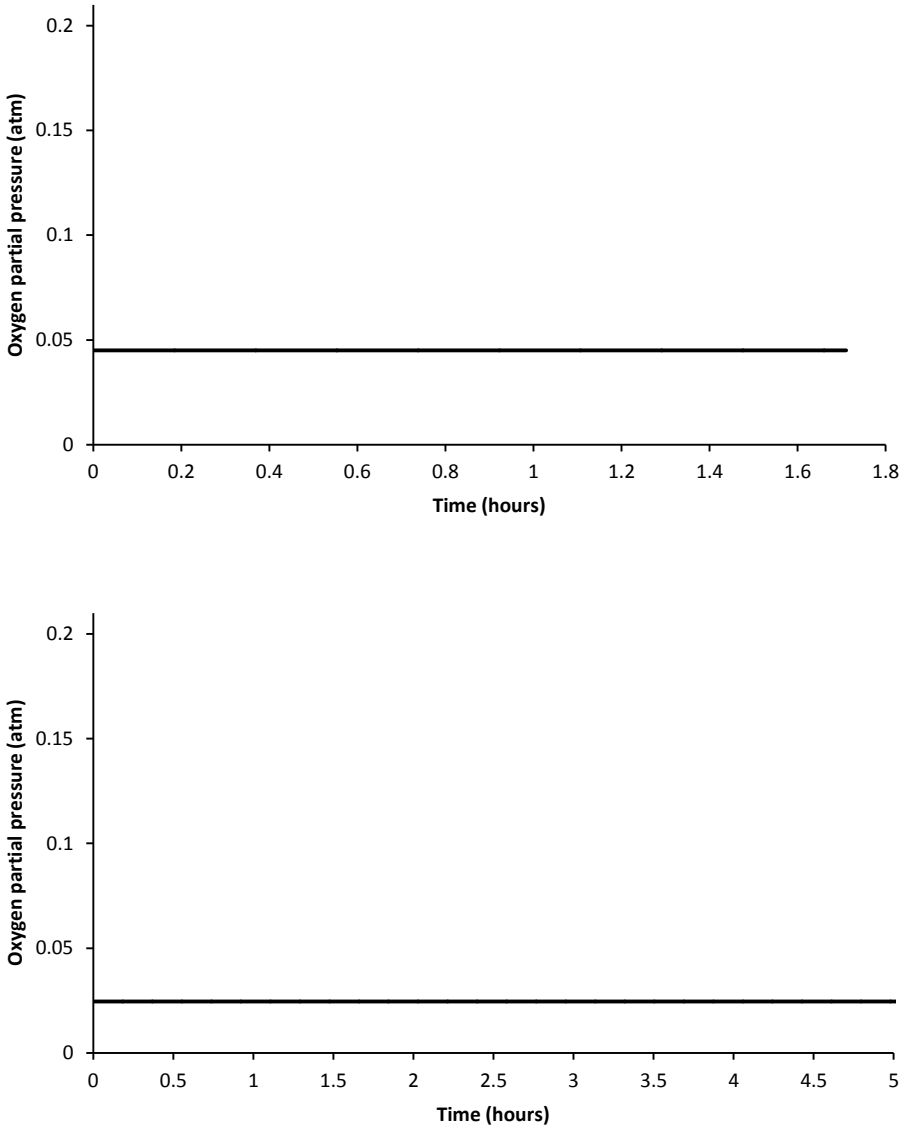

Figure 4.7 The oxygen partial pressure in the respirometer as a function of time in two replicate measurements.

The results show the initial oxygen partial pressure in the samples were slightly higher than zero, which suggested that the oxygen contamination took place as the nitrogen-saturated samples were loaded into the respirometer. This observation was consistent for all replicate measurements which all exhibited similar initial values of oxygen partial pressure. In any case, the initial partial pressure levels are not important for these experiments provided they are low enough to provide a substantial driving force for oxygen transport with the ambient environment (the partial pressure of oxygen in the surrounding water was atmospheric, ~ 0.21 atm).

The results show that the initial values were consistently sustained over considerable time periods. This demonstrates that the respirometer is sufficiently impermeable to oxygen and hence suitable for the purposes of this work.

4.6 Conclusion

This chapter has resolved a number of issues associated with the previous respirometer. As such, the new respirometer should now be technically capable of measuring the oxygen consumption rate of granuloasa cells providing the problems associated with cell death and clumping can now be overcome. These issues are addressed in the next chapter.

Chapter 5. Methodology for granulosa cell harvest

The progress of this study was initially obstructed by the defects in the preliminary respirometer and the observed cell death during measurement. The issues associated with defective respirometer design were addressed in the previous chapter via the development of a new respirometer, which performed well in testing. This work now aims to ensure the viability of granulosa cells during measurement, which will be the subject of this chapter.

Selecting appropriate techniques for handling/processing of ovaries, follicles and granulosa cells are likely to be a key to avoid the cell death observed in previous experiments. In order to achieve this, the techniques for such processing are revisited in great detail. Thus, this chapter will commence by describing the previous methodology which was used for harvesting granulosa cells in the Chapter 3. The issues in the previous procedure will be presented and discussed, and then new methodology for harvesting/handling granulosa cells, which should resolved previous issues and help the granulosa cells to sustain their viability during measurement, will be developed.

5.1 Examination of the previous methodology for granulosa cell harvest

5.1.1 Ovarian collection

Bovine ovaries were collected from cows post mortem at a local abattoir. Typically 30 ovaries were collected per visit and subsequently placed into an insulated flask containing warm isotonic solution (0.9% Sodium Chloride, at 36 to 37℃). The time elapsed between collection of the first ovary and return to the laboratory was approximately 2 hours.

Figures 5.1 and 5.2 show a collection of ovaries and a typical ovary after transportation to the laboratory respectively.

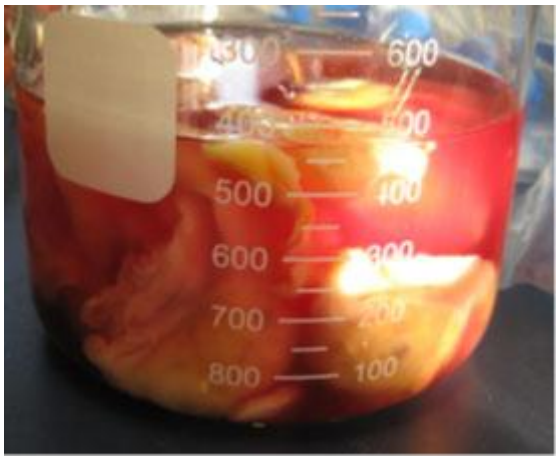

Figure 5.1 The ovarian collection removed from the insulated flask after the transportation from the abattoir.

As Figure 5.1 shows, the saline solution was colored to red by blood. Thus, the ovaries were washed with 0.9% prewarmed ammonium chloride at 37℃to remove blood.

The blister-like features on the surface of the ovary are antral follicles (Figure 5.2, circled).

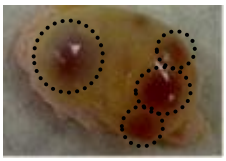

Figure 5.2 An ovary. Showing some of the antral follicles circled with a dotted line.

The four large circled antral follicles in Figure 5.2 are clearly visible from the surface of the ovary. At this point in the experimental methodology, the granulosa cells were harvested by extracting them from their location on the internal wall of such antral follicles (granulosa cell harvest techniques are detailed below).

Previously, the differences regarding the temperature used for transporting ovaries by various studies in the literature was presented (see Section 2.5.1). Some research proposed transporting ovaries in cold conditions and others in warm conditions. Given that cold condition may slow down the metabolic activities in ovarian cells, which could affect their respiratory rate, perhaps even after rewarming, this work chose to use warm conditions to transport ovaries. The range of 36-37℃ used for transportation in this work is close to the temperature *in vivo*. Hence, the effect on the respiratory rate of ovarian cells caused by the temperature is minimized during the transport.

5.1.2 Approaches for granulosa cell harvest

The two general approaches for granulosa cell harvest were compiled in the literature review (see Section 2.5.3). In order to choose a suitable one, this experimental work tested both approaches.

The first approach to granulosa cell harvest required individual follicles to be isolated from the ovary. The ovary was initially dissected into large portions with a scalpel, and then individual follicles were isolated from ovarian tissue using surgical scissors. The outer surface of isolated follicles were subsequently cut and inverted. The granulosa cells were harvested by gently sweeping the internal follicular wall with the back of a scalpel blade.

The second approach was much simpler. Follicles which were visible from the surface of the ovary were ruptured by a 25-gauge needle, and then the follicular fluid was aspirated into a collection vial via application of a vacuum. This process of aspiration harvests granulosa cells as a portion of the cells exit the follicle with the aspirated follicular fluid and can be subsequently recovered from the collection vessel.

5.1.3 Issues associated with each approach to granulosa cell harvest

In this experimental work, the first approach resulted in the emergence of blood in the granulosa cell collection. This is potentially problematic since, unless removed, red blood cells will also consume oxygen in the respirometer. The observed blood might be derived from ruptured capillaries on the surface of follicles as the internal follicular wall was swept by a scalpel or as the follicles were cut from the ovarian tissue.

The second approach did not require ovarian dissection. As a result, the granulosa cells could only be harvested from the follicles which were clearly visible at the surface of ovaries (Figure 5.2). In addition, the aspiration could only extract a small amount of granulosa cells from the follicular wall. Thus, in comparison with the first approach, this approach might result in an insufficient number of granulosa cells for measurement. However, compared with the first method, the needle penetration used in the second approach effectively avoids rupturing the vessels in the follicular surface. Thus, the risk for the blood contamination was significantly reduced.

Blood contamination during granulosa cell collection is a common problem reported by numerous studies. To remove blood, various chemical/physical techniques can be used (see Section 2.5.3). However, such chemical treatments in particular may affect the viability and respiration of granulosa cells. For this reason, in this work, it was deemed preferable to avoid blood contamination rather than remove the blood from the granulosa cell collection with a chemical reagent. Thus, the second approach was more suitable for granulosa cell harvest in this work, provided a sufficient number of granulosa cells could be obtained.

5.2 New methodology development for granulosa cell harvest

5.2.1 New requirements and proposal for the new methods

Based on the above discussion, this work implemented the aspiration method for granulosa cell harvest even though issues associated with granulosa cell scarcity may arise. Although needle penetration followed by aspiration effectively avoids rupturing the capillaries as the granulosa cells are harvested, the emergence of blood in the granulosa cell collection still occasionally occurs. This ruins the collection and aggravates the problem of any potential shortage of granulosa cells. Thus, any proposed new methodology must minimize the risk of granulosa cell contamination by blood.

Along with this issue, the results presented in chapter 3 suggested that the failure to culture cells in the required conditions was the likely cause of the granulosa cell clumps which were deemed to be the likely cause of the observed cell death during measurement. Thus, the new approach also needs to include a method for cell dispersion and clump prevention so that a single granulosa cell suspension can result from harvest.

Further improvement of the granulosa cell harvest and culture conditions will be made by using Medium 199 (M199) instead of the DMEM used in previous experimental work as the granulosa cell culture medium. Compared with the DMEM solution, the M199 has several advantages for culturing granulosa cells. Firstly, M199 contains Hepes which buffers the pH change caused by cell respiration during measurement. Next, Tween 80 is one of the components in M199, which can help with cell dispersion. Also, according to the literature review (see Section 2.5.4.2), M199 is the most common medium for culturing granulosa cells, and was the media used in the previously reported measurements on the oxygen consumption rate of ovine granulosa cells (Gosden & Byatt-Smith 1986).

The following sections aim to develop new methodology to overcome these issues by examining available information on cell dispersion/clump prevention and addressing any issues surrounding a potential granulosa cell shortage arising from the selected technique for extracting these cells from follicles.

5.2.2 Review of granulosa cell dispersion and prevention of granulosa clump formation

Various methods for granulosa cell dispersion as well as the prevention of clump formation are reported in some studies involving granulosa cells.

The simplest method of cell dispersion is to use a micropipette or syringe to repetitively suck the granulosa cells in and out of the opening of the micropipette or syringe to mechanically disperse the granulosa cells (Vanderhyden *et al.* 1992; Van Blerkom *et al.*1997; Clark 2008).

Furthermore, some researchers supplement Heparin into the granulosa cell collection to prevent clump formation (Basini *et al.* 2004; Basini & Tamanini 2000; Metcalf 1982).

Alternatively, the granulosa cells can be dispersed by gently stirring them in a Hanks'-Hepes buffer for 7 min (Yada *et al.* 1999). Basini & Tamanini (2000) dispersed the granulosa cells by culturing them in DNase at 37°C for 15 min.

Unfortunately, no studies have examined the effect of dispersion techniques on cell viability and hence it remains unknown if any of these treatments have adverse effects on culture. In any case, this work will use the most common approach, which is to mechanically disperse the granulosa cells by micropipette or syringe first, with subsequent addition of Heparin to prevent the clump formation.

5.2.3 New methodology for granulosa cell harvest

In this work, a small amount of M199 (approximately 3ml) (Life Technologies Corporation, Auckland, New Zealand, product no. 12340030) supplemented with Heparin (50IU/ml) (SERVA Electrophoresis, Heidelberg, Germany, product no. 24590.02) was loaded into a 10ml syringe equipped with a 25-guage needle. The 25-gauge needle was then used to penetrate the surfaces of large visible follicles on the surface of the ovary and the follicular fluid aspirated by drawing it into the syringe. During this process, the granulosa cells are also drawn into the syringe and subsequently mix with the M199. The mixture was then placed into 1.5ml tubes and placed in a water bath at 37℃. This method was repetitively applied to all large visible follicles to collect the follicular fluid and granulosa cells. The end result of this process was a large number of tubes (typically 40 to 60), each containing a relatively low number of granulosa cells.

At this point the granulosa cells must be concentrated within the media before measurement in the respiration chamber can take place. This is necessary so that drops in oxygen partial pressure are sufficiently large to be detected by the optical probe in a relatively short time frame.

To achieve this, the tubes containing granulosa cells were exposed to centrifugation (800g for 2 min at 37℃ for each run). During each centrifugation run, the granulosa cells settled at the bottom of the media in each tube. After discarding the top 80% of supernatant, the granulosa cell sediment with the remaining medium was repetitively drawn in and out of the opening of 25-gauge needle attached to a 10ml syringe to thoroughly mix the cells within the medium. This process of centrifugation and dispersion was repeated until the granulosa cells became sufficiently concentrated within the media. This process takes between 2-3 hours.

5.3 Conclusion and discussion

The new method described above is expected to result in the concentration and dispersion of granulosa cells ready for measurement in the new respirometer. If the granulosa cells in the suspension are detached, alive and sufficiently concentrated, then they should perform well in the new respirometer system (i.e. a detectable decline in oxygen partial pressure should be measurable), provided they remain viable during the course of the experimental run. The quantity of cells and viability in this suspension can be examined under a microscope after measurement.

One of the improvements in the new method is the use of 1.5 ml tubes to hold the harvested granulosa cells. Using smaller tubes minimizes granulosa cell loss as a result of blood contamination. This is important since, although the aspiration method is scrupulously applied to each follicle, the emergence of blood still occasionally occurs in the granulosa cell collection, which is evidenced by a red color in the granulosa sediment after centrifugation (Figure 5.4).

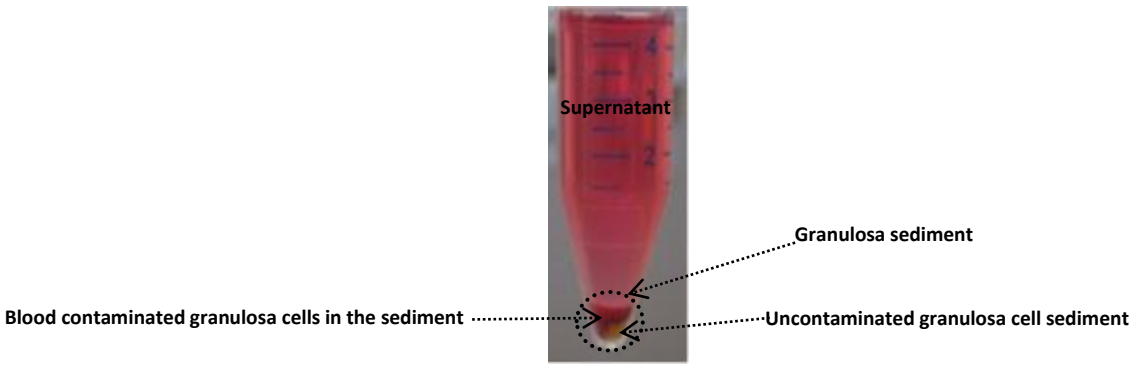

Figure 5.4 The granulosa cell collection after centrifugation (in a 10ml tube). Where, part of the granulosa sediment is colored red by blood.

Previously, 10ml tubes were used to collect the follicular fluid aspirated from follicles. This resulted in a relatively large amount of granulosa cells being accumulated in one tube. Hence, in the case of blood contamination a relatively large number of granulosa cells needed to be discarded. The use of smaller tubes (1.5ml) means that even if blood contamination appears in the sediment, the discarded granulosa cell collection is much smaller, hence less cells are wasted.

According to observations made during this experimental work, application of the aspiration method to large follicles (typically > 5mm in diameter) has less chance of rupturing capillaries. As a result, to alleviate potential granulosa cell shortage, abundant ovarian collection in the abattoir is required (more than 30 ovaries for each collection) and allows larger follicles to be targeted for cell harvest.

Chapter 6. Experimental study of the oxygen consumption rate of granulosa cells

Both the granulosa cell culture conditions and respirometer functionality now meet the specifications required. Therefore, new attempts to measure the oxygen consumption of granulosa cells can be made using the new respirometer. This chapter outlines the work done to characterise the oxygen consumption rate of bovine granulosa cells using the redesigned respirometer and cell culture methodology described in previous chapters.

6.1 Methodology

Before each measurement run, bovine ovaries were collected from cows post mortem at a local abattoir. Typically 30 ovaries were collected per visit and subsequently placed into an insulated flask, containing isotonic solution (0.9% Sodium Chloride, at 36 to 37℃). Ovaries were transported as rapidly as possible to the laboratory after collection.

Follicles (typically > 5mm in diameter) were aspirated with a 10 ml syringe equipped with a 25 gauge needle. The syringe was preloaded with approximately 3 ml of prewarmed M199, containing 50IU/ml Heparin. All of the harvested fluid was then centrifuged at 800g for 2 min at 37℃ to isolate the granulosa cells. Cell dispersion was carried out after each centrifugation run.

This harvesting process resulted a 1.5ml granulosa cell suspension which contained all of the granulosa cells harvested from follicles (detailed the description of cell harvest sees Section 5.2.3). Initial tests showed that the cells collected in this way were sufficiently dispersed and cell viability remained stable during the course of experimental runs. As a result this work measured the cell viability only after each experimental run and assumed that this was the same as the initial cell viability (see discussion for further justification in Section 6.2).

Each measurement run was carried out in the new respirometer described in Section 4.4. A single 1.5ml granulosa cell suspension was placed into the respiratory chamber (2ml vial, equipped with a magnetic stirrer), and supplemented with M199 to fill the 2ml chamber. The chamber was then sealed.

The tip of optical probe was then inserted into the pre-ruptured opening of the septum (for detailed description of the assembly of the new respirometer see Chapter 4.4), and the chamber was inverted to see if any undesirable air bubbles were trapped in the chamber (if air bubbles were observed the chamber was repeatedly resealed until this was no longer the case). Finally, the respirometer was immersed into the water bath at 37℃, and the stirring mechanism of the magnetic stage activated. At this point measurement started and the oxygen partial pressure within the granulosa cell suspension was continuously monitored.

Measurements were carried out on 5 separate occasions. Each measurement involved a separate visit to the local abattoir.

At the end of each measurement run, the granulosa cell suspension in the respiratory chamber was mixed with an equivalent volume of 0.4% Trypan blue and the mixture was incubated in a water bath at 37℃ for a period of 4 min to stain the dead cells. While gently shaking the mixture, the sample in the mixture was then pipetted onto a hemocytometer. The viable cell number in each grid of the hemocytometer was visualized under a microscope at 400 magnifications and used to determine the portion of viable cells in the suspension.

6.2 Results and discussion

Figure 6.1 shows oxygen consumption profiles collected from the five replicate measurement runs in the respirometer.

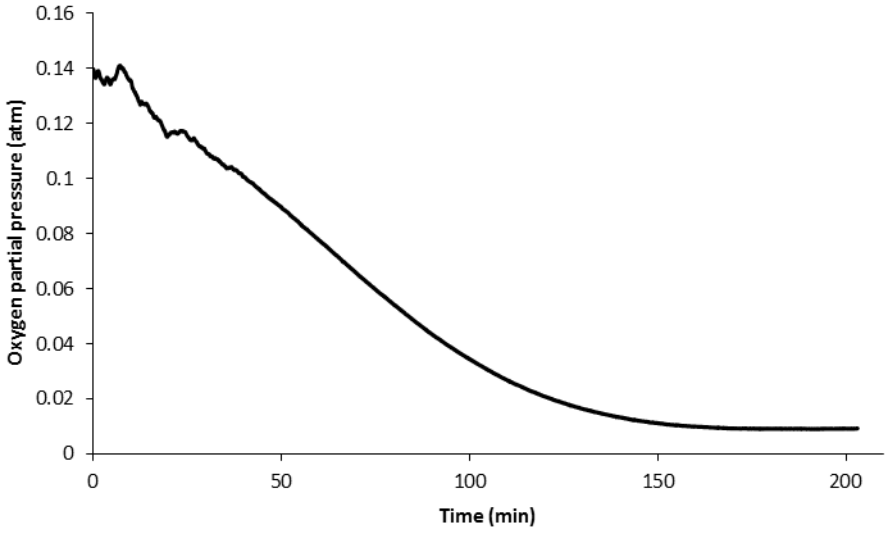

(a) Viable cell concentration 8.0 x 10^4 cell/ml

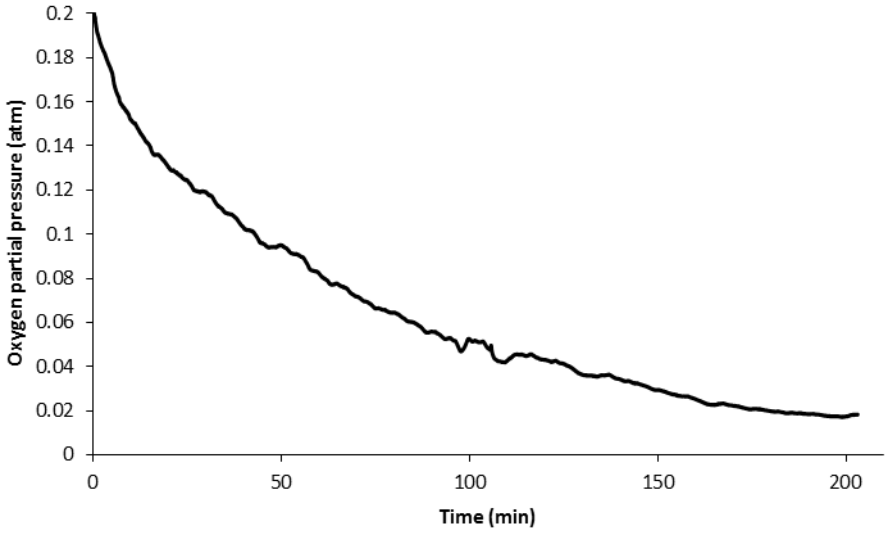

(b) Viable cell concentration 2.2 x 10^5 cell/ml

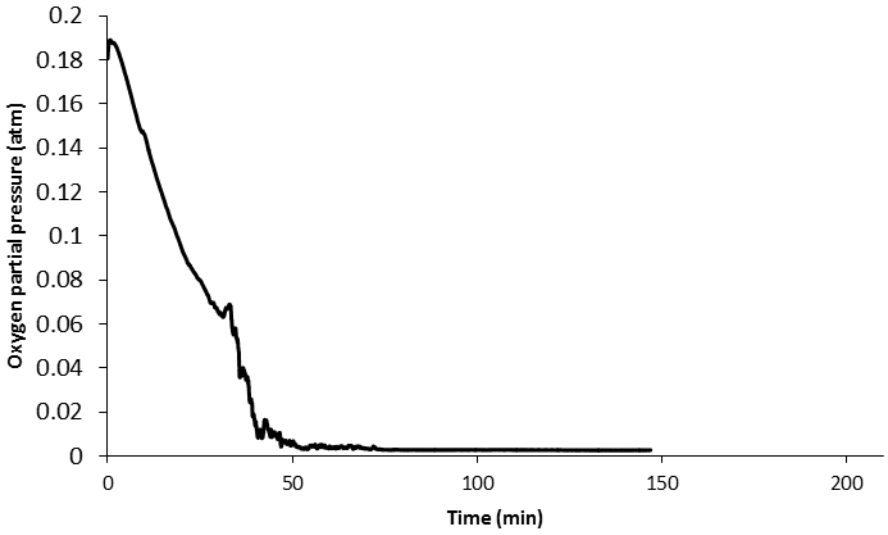

(c) Viable cell concentration 2.2 x 10^5 cell/ml

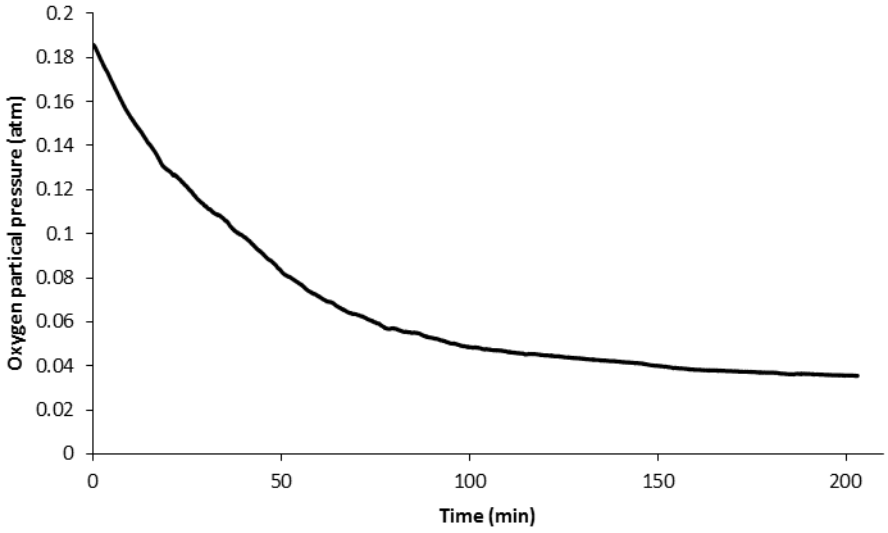

(d) Viable cell concentration 2.0 x 10^5 cell/ml

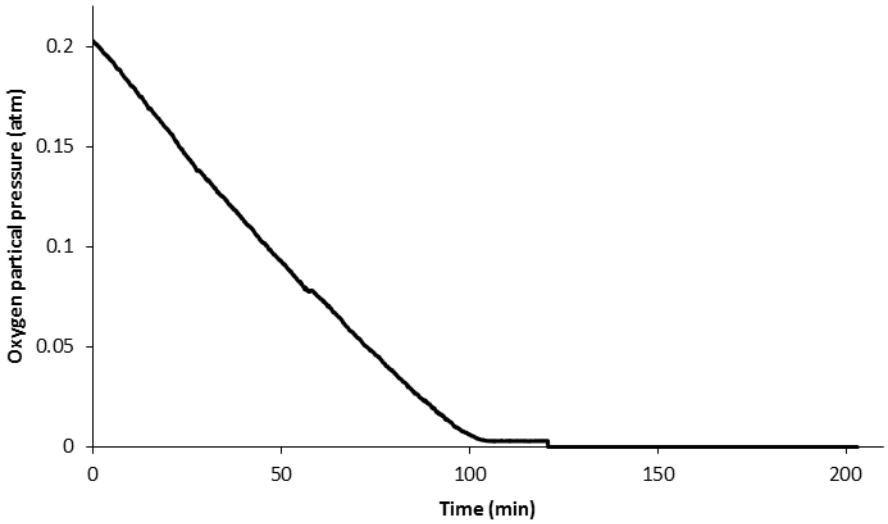

(e) Viable cell concentration 1.7 x 10^5 cell/ml

Figure 6.1 Oxygen partial pressure in the granulosa suspension as a function of time (min) in each measurement run which is labelled by (a), (b), (c), (d), (e) respectively. Where the cell concentration is given under each of the consumption profiles.

As the results in Figure 6.1 show, the initial 0.05 atm drop in oxygen partial pressure for each measurement run was approximately linear. The period of linear decrease represents a period of constant oxygen consumption rate by the granulosa cells. The curved portion of the data represents a non-constant oxygen consumption rate. There may be a number of reasons why the oxygen consumption rate becomes non-constant and these are discussed later.

The cell concentration was determined by cell count at the end of each measurement run. According to the observations under the microscope, the granulosa cells were partially dispersed and the stained cells were less than 10% in each measurement run (i.e. all runs had greater > 90% viability).

Note that the possibility of cell proliferation during the measurement was not investigated by this experimental work. According to the literature, the proliferation of granulosa cells requires the oocyte-secreted paracrine (Li *et al.* 2000). The absence of the oocyte in these measurements makes such cell increase unlikely. Based on the high viability (>90%) and unlikely proliferation, this work assumed that the cell number in each run was constant (at the number determined at the end of the experimental run) during the initial period of linear decrease. This period was taken as time period over which the respiration of the cells resulted in the 0.05 atm drop in oxygen partial pressure.

This assumption also neglects the possibility of cell death over the course of each experimental run. Since all post run cell viabilities were >90% this will result in a worst case under estimate of 10% in the viable cell count (i.e. if all cells were in fact viable at the initiation of the experimental run). The calculations detailed below show that both the calculation of cellular oxygen consumption rate on per cell and per volume basis are proportional to the inverse of the viable cell number. Hence, the possible underestimation of viable cell numbers

will lead to a worst case error in cellular oxygen consumption rate of (1 – (1/0.90)) x 100 = 11%. That is, in the worst case cellular oxygen consumption rate will be overestimated by 11%. This is deemed acceptable to this work and is likely smaller than the errors associated with determining cell numbers.

Based on the above results and discussion, Table 6.1 was constructed to show quantitative information which describes the initial 0.05 atm oxygen partial pressure drop caused by the granulosa cells in each measurement run.

Run	Time for 0.05 atm drop (min)	Viable cell conc. (cell/ml)
1	50	8.0×10^4
2	11	2.2×10^5
3	13	2.2×10^5
4	17	2.0×10^5
5	22	1.7×10^5
Range	11 to 50	0.80 to 2.2×10^5

Table 6.1 Time for 0.05 atm drop and the corresponded cell concentration in each measurement run.

The linear region extended down to very low oxygen concentrations for three of the measurement runs (a, c and e). However, curved portions appeared in the profiles for the measurements of (b) and (d), suggesting non-constant oxygen consumption rates after the initial periods. One possible reason might be that the cells are displaying Michaelis-Menten type kinetics though if this were true a non-linear region would be expected for all curves. Other reasons may include nutrient depletion and cell death during these experimental runs. However, since such variables were not controlled in this work it is impossible to determine the exact cause of the curvature.

In general, the oxygen consumption rate of animal cells is constant and only becomes non-constant as the oxygen drops to hypoxic levels (Braems & Jensen 1991; Clark 2008). Note the oxygen consumption profile of ovine granulosa cells given by Gosden & Byatt-Smith (1986) fits this description well.

The oxygen consumption rate of granulosa cells is of particular interest because it dictates the intrafollicular oxygen levels across follicle (see Introduction). According to the research conducted by Redding 2007; Clark 2008, the inclusion of the non-constant rate at hypoxic levels only has an insignificant effect on oxygen transport in follicles. As a result of the above this work is concerned only with estimating the constant rate oxygen consumption of granulosa cells and this is achieved by using only the initial 0.05 atm drop for all experimental runs.

6.3 The oxygen concentration in granulosa cell suspension

The oxygen partial pressure in cell suspension can be related to the oxygen concentration by Henry law.

$$C(O_2)= p(O_2)\times S(O_2) \quad (6.1)$$

Where $C(O_2)$ is oxygen concentration ($mol.m^{-3}$), $p(O_2)$ is oxygen partial pressure (mmHg), $S(O_2)$ is oxygen solubility ($mol.m^{-3}.mmHg^{-1}$).

Gnaiger (2010) suggested that solutes only slightly affect the oxygen solubility in pure water at 37℃. Furthermore, the concentrations of various solutes in M199 are really low (approximately 17g solutes in total/L). The higest solute concentration is that of NaCl at 6.1 g/L. Therefore, this work assumes that the solubility of M199 equal to the solubility of salt solution (6.1g/L) at 37 ℃, which was estimated to be 94% of the solubility of pure water at 37 ℃ (Hitchman, 1978). This gave a value of 0.00129 $mol.m^{-3}.mmHg^{-1}$.

Having determined the oxygen solubility in the respirometer media the measured partial pressures can be easily converted to concentration via equation 6.1.

6.4 The oxygen consumption rate of granulosa cells and comparison with oxygen concentration rate of other animal cells

Based on Table 6.1, the oxygen consumption rates determined from each measurement run on both a per cell and volumetric basis are given by Table 6.2. To facilitate the calculation of these rates, the observed partial pressure drop (0.05 atm) has been converted to the corresponding oxygen concentration change (0.049 mol/m^3).

Run	Time for 0.049 mol/m^3 oxygen concentration drop (min)	Viable cell conc. (cell/ml)	Oxygen Consumption Rate ($mol.cell^{-1}.s^{-1}$)	Oxygen Consumption Rate ($mol.m^{-3}.s^{-1}$)
1	50	8.0×10^4	2.1×10^{-16}	0.16
2	11	2.2×10^5	3.3×10^{-16}	0.25
3	13	2.2×10^5	2.9×10^{-16}	0.22
4	17	2.0×10^5	2.4×10^{-16}	0.18
5	22	1.7×10^5	2.2×10^{-16}	0.16
Range	11 to 50	0.80 to 2.2×10^5	2.1 to 3.3×10^{-16}	0.16 to 0.25

Table 6.2 Per cell and volumetric granulosa cell oxygen consumption rates

The oxygen consumption rate in each measurement run is expressed in terms of $mol.cell^{-1}.s^{-1}$ and $mol.m^{-3}.s^{-1}$. These values are calculated by equation 6.2 and 6.3 respectively.

$$R_g = \frac{\Delta C}{\Delta t C_{cell}} \quad \left[\frac{mol}{cell.s}\right] \tag{6.2}$$

$$R_g = \frac{\Delta C}{\Delta t C_{cell} V_{cell}} \quad \left[\frac{mol}{m^3.s}\right] \tag{6.3}$$

Where, R_g is the oxygen consumption rate of granulosa cell (mol.cell^{-1}.s^{-1} or mol.m^{-3}.s^{-1}). ΔC (0.049 mol.m^{-3}) is the concentration drop in the granulosa cell suspension which occurred over time Δt (s). The time, Δt, taken for this drop is given in Table 6.2 for each run. C_{cell} (cell.m^{-3}) is the viable cell concentration in the granulosa cell suspension, given in Table 6.2 for each run. V_{cell} (1.32×10^{-15} m^3) is the volume of a single granulosa cell. This was calculated from the granulosa cell diameter observed under microscope at 1000 magnifications by this work at the end of each measurement run. Under observation, most of the granulosa cells appeared spherical in shape, and their diameters ranged from 0.012 mm to 0.015 mm. The median diameter value (0.0135 mm) was used for this calculation.

Table 6.3 compares the granulosa oxygen consumption rates determined in this work with various other cellular oxygen consumption rates reported in the literature for a variety of cell types.

Cell type	Oxygen Consumption Rate	Reference
CHO (Chinese hamster ovary) cell	0.254-0.28	Ducommun *et al.* (2000)
Myeloma	0.219-0.406	Ruffieux *et al.* (1998)
Guinea pig fetal muscle cell	0.4	Braems & Jensen (1991)
Hybridoma	0.41-0.51	Ruffieux *et al.* (1998)
Bovine granulosa cell	0.74-1.20	This work (2012)

Table 6.3 Oxygen consumption rates of various animal cells compared to bovine granulosa cells. All consumption rates have units of ×10^{-12} mol O_2/cell/h.

Table 6.3 demonstrates that although comparable with other cell types, the rate range of oxygen consumption by bovine granulosa cells appears the highest value among these animal cells. Furthermore, the rate of oxygen consumption by ovine granulosa cells is 0.0363 mol.m^{-3}.s^{-1} (Gosden & Byatt-Smith 1986) which is approximately 5 times lower than the rate value of bovine granulosa cells (0.16 to 0.25 mol.m^{-3}.s^{-1}) given by this work.

6.5 Conclusion

The oxygen consumption rates of granulosa cells were successfully measured under the desired conditions set out in previous chapters. A period of linear decrease in oxygen partial pressure occurred in the initial period of each experimental run and was used to calculate the oxygen consumption rate of the granulosa cells. The cellular oxygen consumption rates determined in this work were comparable with but higher than those reported for other cell types. Furthermore, the oxygen consumption rate of bovine granulosa cells reported here was approximately 5 times higher than the rate of ovine granulosa cells.

Literature investigations into the oxygen levels across follicles have been previously conducted based on the oxygen consumption rate of ovine granulosa cells (see Introduction). The results of such studies showed that oxygen transport across the follicle was strained by severe oxygen depletion in the granulosa layer. Intrafollicular hypoxia was shown to be inevitable as the follicle grew beyond a certain threshold size.

Thus, it is interesting to consider what the implications of the faster rate of oxygen consumption reported in this work may have on oxygen transport in the ovarian follicle. The next chapter will apply the data collected here to an existing model to investigate the impact of the oxygen consumption rates measured in this work on the oxygen levels across the follicle.

Chapter 7. Oxygen transportation in bovine follicles

The previous chapter measured bovine granulosa cell oxygen consumption rates that were approximately 5 times faster than the values reported by Gosden & Byatt-Smith (1986) for ovine granulosa cells. Taken in isolation this would suggest that oxygen transport in follicles may be even more strained than previous studies report. However, the models used to study the oxygen transport across follicles (Gosden & Byatt-Smith 1986; Redding *et al.* 2007) have more parameters than just oxygen consumption rate and these must also be considered before any conclusions can be drawn.

The key parameters in these models include granulosa cell oxygen consumption rate, follicular fluid content (see Section 2.2.4) of the granulosa layer and oxygen content at the follicle surface, as well as the geometric parameters of the follicle. In existing studies these parameters have been estimated from a variety of sources, across a variety of species. How sensitive these models are to species specific parameter estimates remains unknown and represents uncertainty in the reliability of such model predictions.

Large preantral follicles are of particular interest because the models suggest that oocytes in large preantral follicles would be exposed to severe hypoxia (Gosden & Byatt-Smith 1986). Subsequent studies have suggested that the oocyte is first exposed to severe hypoxia in late preantral follicles, just before antrum formation begins which is favourable to intrafollicular oxygen content, resulting in higher oocyte oxygenation (Redding *et al.* 2007, 2008). This is consistent with measured oxygen content in bovine antral follicles, which is 0.07 atm given by De Castro e Paula *et al.* (2008).

The objectives of this chapter are to examine the oxygen consumption rate data obtained in the previous chapter in the context of oxygen transport in large bovine preantral follicles. This includes description of species specific parameter estimates for use in mathematical models of oxygen transport in large bovine preantal follicles. These parameter estimates are then used to predict the oxygen levels in large bovine preantral follicles and the results discussed in relation to follicle hypoxia.

7.1 Methodology

7.1.1 Mathematical model

The equation used to predict the oxygen concentration at any position across a preantal follicle is that described Redding *et al.* (2006). This is a modified version of that used by Gosden and Byatt-Smith (1986) for predicting oxygen levels in preantral follicles.

$$C = C_o - \frac{R_g(1-\varepsilon)}{6D_{eff}}\left(r_f^2 - r^2\right) for\ 0 \le r \le r_f \quad (7.1)$$

$$If\ C < 0, then\ C = 0\ (concentration\ cannot\ be\ negative)$$

Where

C - oxygen concentration at any position along the radius of the follicle (mol.m^{-3})

C_o - oxygen concentration at the surface of follicles (mol.m^{-3})

R_g - oxygen consumption rate of per unit volume of granulosa cells (mol.m^{-3}.s^{-1})

ε - volume fraction of fluid in the granulosa layer

D_{eff} - diffusion coefficient of oxygen in the granulosa layer (m^2.s^{-1})

r_f - follicle radius (m)

r - the radial distance from the follicle centre (m)

The model is based on a number of assumptions. Firstly, the oocyte is assumed to have the same properties as granulosa layer. In other words, the oocyte is excluded from this model. Next, the preantral follicle is assumed to be spherical, and composed of granulosa cells and follicular fluid which fills the space between the granulosa cells. Oxygen transport in the follicle is assumed to be via diffusion and the rate of oxygen consumption by granulosa cells is assumed to be constant. No oxygen is consumed in the fluid. Hence the fluid voidage facilitates oxygen transport across the follicle. The follicle surface is assumed to be completely vascularised. The oxygen concentration at follicle surface is assumed equal to the concentration in arterial blood and to be uniform across the entire surface.

7.1.2 Parameter estimates

Bovine preantral follicles which fall within a range of 58 to 145μm in radius (r_f) are considered to be large bovine preantral follicles and it is this size range that is considered by this work. The values of the lower and upper ends of this range represent the smallest bovine follicle radius in which the antrum is first observed and the largest bovine preantral follicle radius beyond which the antrum always is observed. Hence, a bovine preantral follicle within this size range is also considered to be in a transitional follicular stage, in which the follicle may or may not have an antrum. The values of the lower and upper ends of the range were given by Monniaux *et al.* (1984) and Lussier *et al.* (1987) respectively. The assumption of complete vascularisation is more likely to be valid in this follicle size range as vascular development is known to maximal during the late preantral and early antral stages of follicular development (Fraser, 2006). The oxygen status of the oocyte will be inferred by assuming it to be centrally located and of radius 34 μm. This is the average oocyte radius reported for large bovine prantral follicles by Braw-Tal & Yossefi (1997).

7.1.2.1 Oxygen concentration at the follicle surface (C_o)

Wagner *et al.* (1990) gave the blood oxygen partial pressure in an adult dairy cow as 109 ± 12 mmHg (mean ± SD). This can be converted to a concentration using Henry's law (see equation 6.1 given in Section 6.3). The oxygen solubility in follicles was considered as constant and equivalent to follicular fluid. This value has been given by Redding *et al.* (2007), as $0.00125 mol.m^{-3}.mmHg^{-1}$. Hence, according to Henry's law, the oxygen concentration follicular surface is $109 \times 0.00125 = 0.136 \pm 0.015$ $mol.m^{-3}$. This work will test the range of mean ± SD.

7.1.2.2 Fluid voidage (ε)

Fluid voidage is the volume fraction of tissue which is occupied by fluid (the rest being occupied by cells).

Serial follicular cross-sections from the work of Braw-Tal & Yossefi (1997) are shown in Figure 7.1. This depicts the morphological changes of the granulosa layer over the primordial to late preantral follicular stages.

When the follicles are in the primordial or early primary stage (Figure 7.1 a, b), the entire granulosa layer is almost entirely composed of tightly packed granulosa cells. As follicles grow the gap between the granulosa cells increases and is filled by follicular fluid. As the follicle grows to the late preantral stage (Figure 7.1 d) the proportional volume of fluid in the granulosa layer increases further. This reveals that as the preantral follicle grows the proportion of the granulosa layer occupied by fluid increases. The importance of the increase in fluid voidage on the oxygen transport has been described in Section 2.3. In order to make

useful predictions using the mathematical model, these quantitative observations regarding fluid voidage need to be quantified.

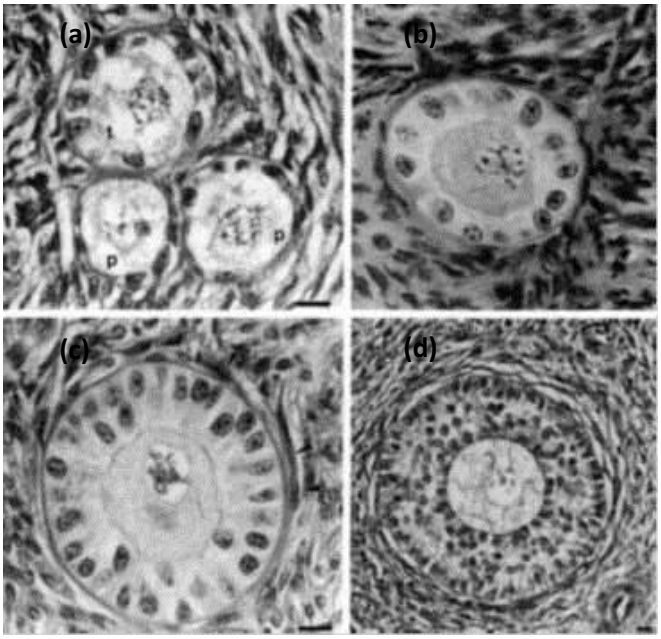

Figure 7.1 The largest cross-sections of various preantral bovine follicles. Where (a) two primordial follicles labelled by **p**; (b) primary follicle; (c) small preantral follicle; (d) large preantral follicle (images taken from Braw-Tal & Yossefi 1997).

Braw-Tal & Yossefi (1997) also reported ranges in the number of granulosa cells in cross sections of follicles of various sizes (all sections were the largest containing the oocyte). For large preantral follicles the cell numbers in such cross sections varied from 101 to 250. The corresponding follicle radii range was 66 to 125 µm. Using these values and assuming low cell numbers correspond to low follicle radii and vice versa, the fluid voidage can be calculated as (assuming follicle, granulosa cells and oocyte to be spherical),

$$\varepsilon = 1 - \frac{n_g \pi r_g^2}{\pi r_f^2 - \pi r_o^2} \qquad (7.2)$$

Where

n_g is the number of granulosa cells in a cross section and r_g, r_f and r_o are the radii of the single granulosa cell, follicle and oocyte respectively. r_o was given above as 34µm. The radius of a single preantral granlulosa cell was estimated from the work of Lussier *et al.* (1987) to be 4.5µm which is consistent with the granulosa size range in the images given by Calado *et al.* (2001).

From these values the fluid voidage was calculated to range of 0.34 to 0.65 (corresponding to the follicle radius range of 66 to 125 µm). The upper end of this range is at the high end of that observed in normal animal tissue but is consistent with images given by Marion *et al.* (1968) of large bovine preantral follicles (Figure 7.2).

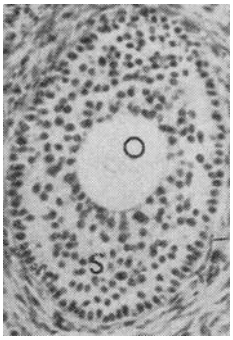

Figure 7.2 A large bovine preantral follicles, where oocyte is labelled by **O**; granulosa layer is labelled by **S** (images taken from Marion *et al.* 1968).

7.1.2.3 Effective diffusion coefficient of oxygen in the follicle (D_{eff})

Diffusion through the follicle will be a result of a combination of diffusion through its cellular and fluid components. An empirical correlation described by Equation 7.3 (Riley *et al.* 1994, 1995, 1996) can be used to calculate the effective diffusion coefficient (D_{eff}) given the values of the diffusion coefficients through the cellular and fluid phases.

$$\frac{D_{eff}}{D_a} = 1 - (1 - \frac{D_g}{D_a})(1.727(1-\varepsilon) - 0.8177(1-\varepsilon)^2 + 0.09075(1-\varepsilon)^3) \quad (7.3)$$

Where

D_a is the diffusion coefficient of oxygen through the follicular fluid and D_g is the diffusion coefficient of oxygen through the granulosa cells. The values of D_g and D_a were also estimated by Redding *et al.* (2007), as 3.0×10^{-10} $m^2.s^{-1}$ and 2.6×10^{-9} $m^2.s^{-1}$ respectively. Hence knowing these values and the fluid voidage for a given follicle, the effective diffusion coefficient of oxygen through the granulosa can be calculated.

7.1.2.4 The oxygen consumption rate of granulosa cells

The oxygen consumption rate of granulosa cells will be assumed to vary across the range reported previously in this work, 0.16 to 0.25$mol.m^{-3}.s^{-1}$ (see Section 6.4).

7.2 Results and discussion

7.2.1 Bovine specific parameter estimates required by the model for predicting the oxygen levels across large preantral follicles.

Fluid voidage ($\mathcal{E}$) values in large preantral follicles are specific to particular follicle sizes. Specifically at r_f = 125µm, $\mathcal{E}$ = 0.65 and at r_f = 66µm, $\mathcal{E}$ = 0.34 (see Section 7.1.2.2). Since D_{eff} is a function of $\mathcal{E}$, it may also be considered to be follicle size specific.

For clarity, each predicted result presented below will specifically indicate the values of r_f, $\mathcal{E}$ and D_{eff} that were used as input parameters to the model.

Other bovine specific parameter estimates are considered in this work to be independent of follicular size across the follicle size range tested. Values for these parameters are summarised in Table 7.1.

Parameter	Units	Value	Reference
r_o	M	34×10^{-6}	Braw-Tal & Yossefi (1997)
C_o	$mol.m^{-3}$	0.121 to 0.151	Wagner *et al.* (1990)
R_g	$mol.m^{-3}.s^{-1}$	0.16 to 0.25	This work (2012)

Table 7.1 Bovine specific parameter estimates used in model predictions.

7.2.2 Oxygen profiles across large preantral follicles

The oxygen concentration in preantral follicle as a function of the radial distance from the follicle centre can be profiled by plotting C vs r after prediction via equation 7.1. Such oxygen concentration predictions are subsequently converted to the oxygen partial pressure via Henry's Law (see equation 6.1 given in Section 6.3).

Figure 7.3 shows the predicted oxygen partial pressure profiles in two large preantral follicles, in which r_f = 66µm; $\mathcal{E}$=0.34; D_{eff} = 7.4×10^{-10} $m^2.s^{-1}$ (Figure 7.3 (a)) and r_f = 125µm; $\mathcal{E}$=0.65; D_{eff} = 1.43×10^{-9} $m^2.s^{-1}$ (Figure 7.3 (b)) respectively. Other parameter estimates are derived from Table 1 and used in the following combinations.

(i) Nominal (mid-range values of C_o and R_g)
(ii) Favourable to oxygen transport (high C_o and low R_g)
(iii) Unfavourable to oxygen transport (low C_o and high R_g)

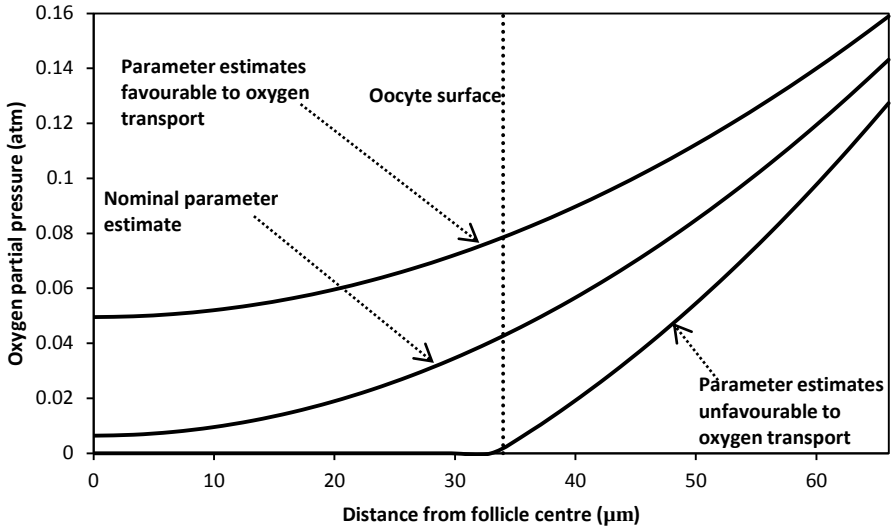

(a) r_f = 66µm; $\mathcal{E}$=0.34; D_{eff} = 7.4×10^{-10} m^2.s^{-1}

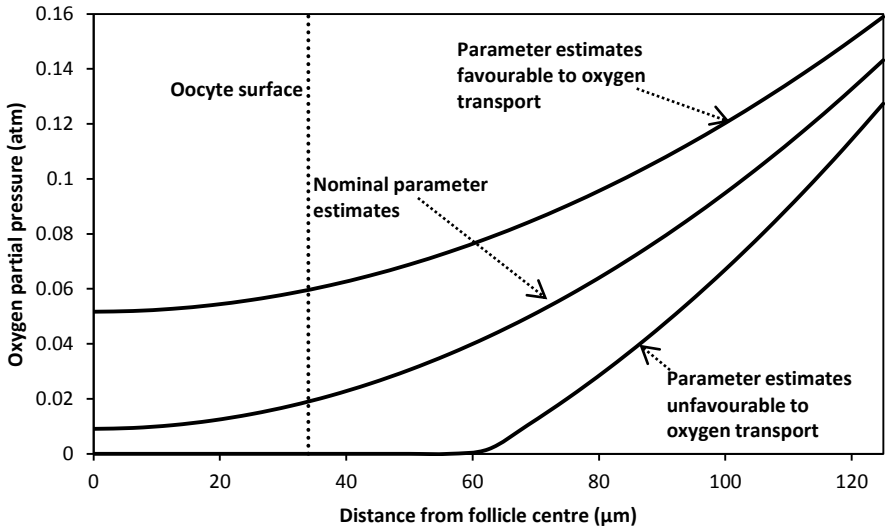

(b) r_f = 125µm; $\mathcal{E}$=0.65; D_{eff} = 1.43×10^{-9} m^2.s^{-1}

Figure 7.3 The oxygen partial pressure profiles across two large preantral follicles. Where locations of oocyte surfaces in these follicles are depicted by the dashed lines.

The predictions give a comparison of the oxygen profiles across follicle of radius 66 µm and 125 µm. The results show that oxygen transport is strained by increasing follicle radius (r_f). At r_f = 66µm, the oxygen reaches the oocyte surface even under the most unfavourable conditions to oxygen transport (although only marginally). At r_f = 125 µm oxygen transport is much more strained. Under unfavourable conditions oxygen falls well short of the oocyte surface and only marginally reaches the oocyte under nominal conditions. Under the most favourable conditions oxygen can still reach the oocyte.

Bovine preantral follicles have been reported to grow as large as 145 µm in radius (Lussier *et al.* 1987). Beyond this radius all follicles are observed to have fluid filled antrums. In follicles of

this size oxygen transport will be further strained. It has been suggested that antrum formation is coincident with oocyte hypoxia and that any growth beyond this size without the formation of the antrum would result in severe oocyte hypoxia for all follicles (Redding *et al.* 2007). If this is the case it would be expected that the predicted oxygen concentration profile across such a follicle would demonstrate oocyte hypoxia even under the most favourable conditions to oxygen transport.

In order to predict such profiles the voidage (ε) in a 145 µm radius follicle must be estimated. This work assumes the ε value in such a large preantral follicle is 0.65, which is the value estimated for a follicle of radius 125 µm. This is likely an estimate as this follicle is only slightly larger than the 125 µm radius for which the voidage has been calculated. Voidage values much larger than this are perhaps unlikely as this appears to be at the upper end of the range expected for animal tissue (Truskey *et al.* 2004). Figure 7.4 shows the oxygen profile across the largest preantral bovine follicle (r_f = 145µm; ε=0.65; D_{eff} = 1.43×10^{-9} $m^2.s^{-1}$; all other parameter estimates were given by Table 1).

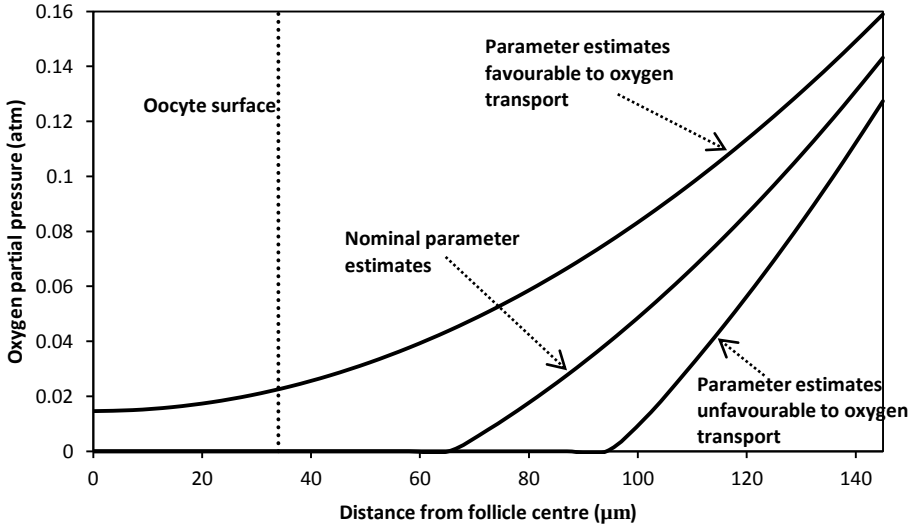

Figure 7.4 The oxygen partial pressure profile across the largest bovine preantral follicle. Where the location of oocyte surface is depicted by the dashed line.

The results Figure 7.4 show that the largest preantral follicle has grown to a size which the oocyte is completely starved of oxygen except under the most favourable conditions. In this case the oocyte surface is still hypoxic at a level of ~ 0.02 atm. This result is consistent with the hypotheses that antrum formation is coincident with sever oocyte hypoxia.

Figure 7.5 shows the same prediction as that of Figure 7.4 but instead using the oxygen consumption rate of ovine granulosa cells, in which R_g = 0.0233-0.0493 mol.m^{-3}.s^{-1} (Gosden & Byatt-Smith 1986).

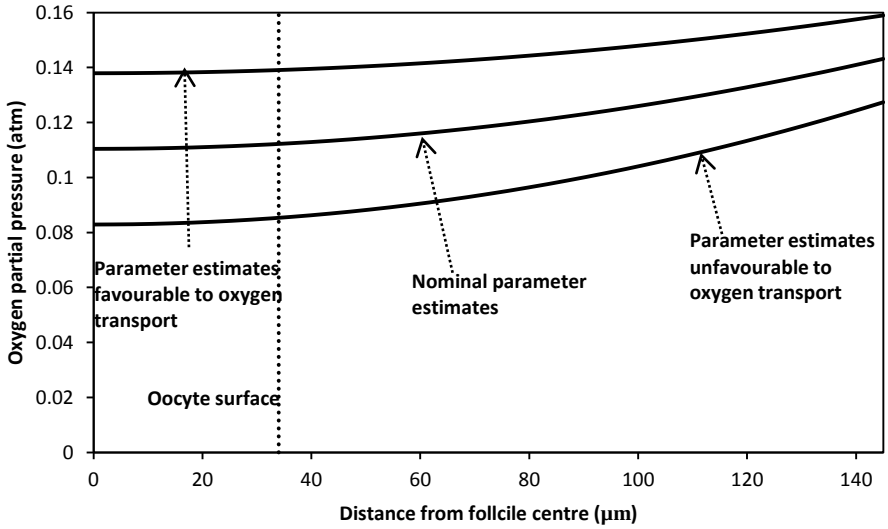

Figure 7.5 The oxygen partial pressure profile across the largest bovine preantral follicle using ovine granulosa cell oxygen consumption rates instead of bovine. Where the location of oocyte surface is depicted by the dashed line.

Figure 7.5 shows that if bovine granulosa cells consumed oxygen at the same rate as that reported for ovine granulosa cells, the oocyte never experiences hypoxia, even under the most unfavourable conditions. This highlights the significance of species specific parameter estimates including the effects of the geometric parameters unique to each species.

For example, the fluid voidage in ovine preantral follicles is much lower than bovine preantral follicles. The highest fluid voidage level of 0.32 was found in large ovine preantral follicles (~170μm in radius) (Redding personal communication). The low fluid voidage and larger follicle size are unfavourable to the oocyte oxygenation. To make a valid prediction, the inclusion of these two ovine specific parameter estimates is important.

The predicted oxygen profiles in the largest ovine preantral follicle are shown in Figure 7.6, in which C_o = 0.136 ± 0.015mol.m^{-3}, R_g = 0.0233-0.0493 mol.m^{-3}.s^{-1}, Ɛ = 0.32, D_{eff} = 7.0 × 10^{-10} m^2.s^{-1}, r_f = 170µm, r_o = 44µm (the oocyte radius in large ovine preantral follicle given by Lundy *et al.* 1999).

Note that in Figure 7.6 the oxygen levels at the follicle surface of sheep follicles has been assumed the same as those used for bovine follicles in this work. The arterial oxygen partial pressure in an adult sheep is 104.4 ± 2.9mmHg (Hales 1973), which is within the range of the blood oxygen partial pressure (109 ± 12mmHg) in an adult dairy cow (see Section 7.1.2.1). Hence this is a reasonable assumption.

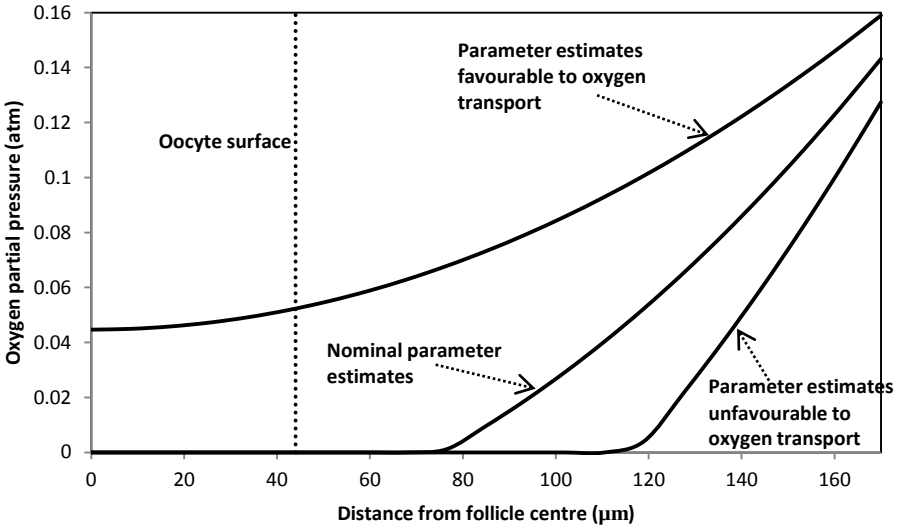

Figure 7.6 The oxygen partial pressure profile across the largest ovine preantral follicle. Where the location of oocyte surface in this follicle is depicted by the dashed line.

This oxygen profile indicates that the oocyte suffers severe hypoxia unless the follicle combines all of the oxygen transport favourable parameter estimates. Even in the case of favourable oxygen transport parameters the oxygen levels at the oocyte surface still only reach ~ 0.05 atm. This result is similar to the oxygen profile for the largest bovine preantral follicle. The similarity shows that some preantral follicles have grown beyond a distance which results in severe oocyte hypoxia.

The results presented here suggest that oxygen transport in bovine and ovine preantral follicles is likely to be the result of a unique combination of parameters for a particular species. In addition to geometric paramters the oxygen consumption rate and fluid voidage of follicles of a given species will be the key determinants in oxygen levels across the follicle. This is because parameters such as oxygen levels in the blood and diffusivity through plasma/follicular fluid are likely to be similar across mammalian species. Hence the oxygen consumption rate and fluid voidage of a particular species largely govern how large the follicle can grow before the oocyte experiences hypoxia.

It is worth noting that although this work used quite a narrow range of species specific parameter estimates, the variability in the predicted ranges are still reasonably wide. Hence the model is very sensitive to variations in parameter estimates (the predictions are approximately equally sensitive variations in C_o, R_g and ε using the parameter estimates described in this work). This also reflects the likelihood that the experience of any given follicle is likely to be unique.

7.2.3 Maximum follicle size and oocyte oxygenation

According to the mathematical model used in this chapter, for any given desired oxygen level at the oocyte there will be a maximum size that the follicle can grow to. Growth beyond this size will dictate that the oocyte can no longer sustain the desired oxygen level. Figure 7.7 can be used to determine the maximum follicle radius at which a follicle can sustain a given level of oxygen at the oocyte surface. Figure 7.7 was produced as follows,

Equation 7.1 was rearranged to make r_f the subject and the radius was set to $r = r_o$. This setup gives equation 7.4, in which C is the oxygen concentration at the oocyte surface (since $r = r_o$). Figure 7.7 was then produced by evaluating equation 7.4 at various values of C and ε. Note that concentrations have been converted to partial pressures for display in Figure 7.7 and that all parameter estimates are at their nominal levels.

$$r_f = \sqrt{r_o^2 + \frac{6D_{eff}(C_o - C)}{R_g(1-\varepsilon)}} \tag{7.4}$$

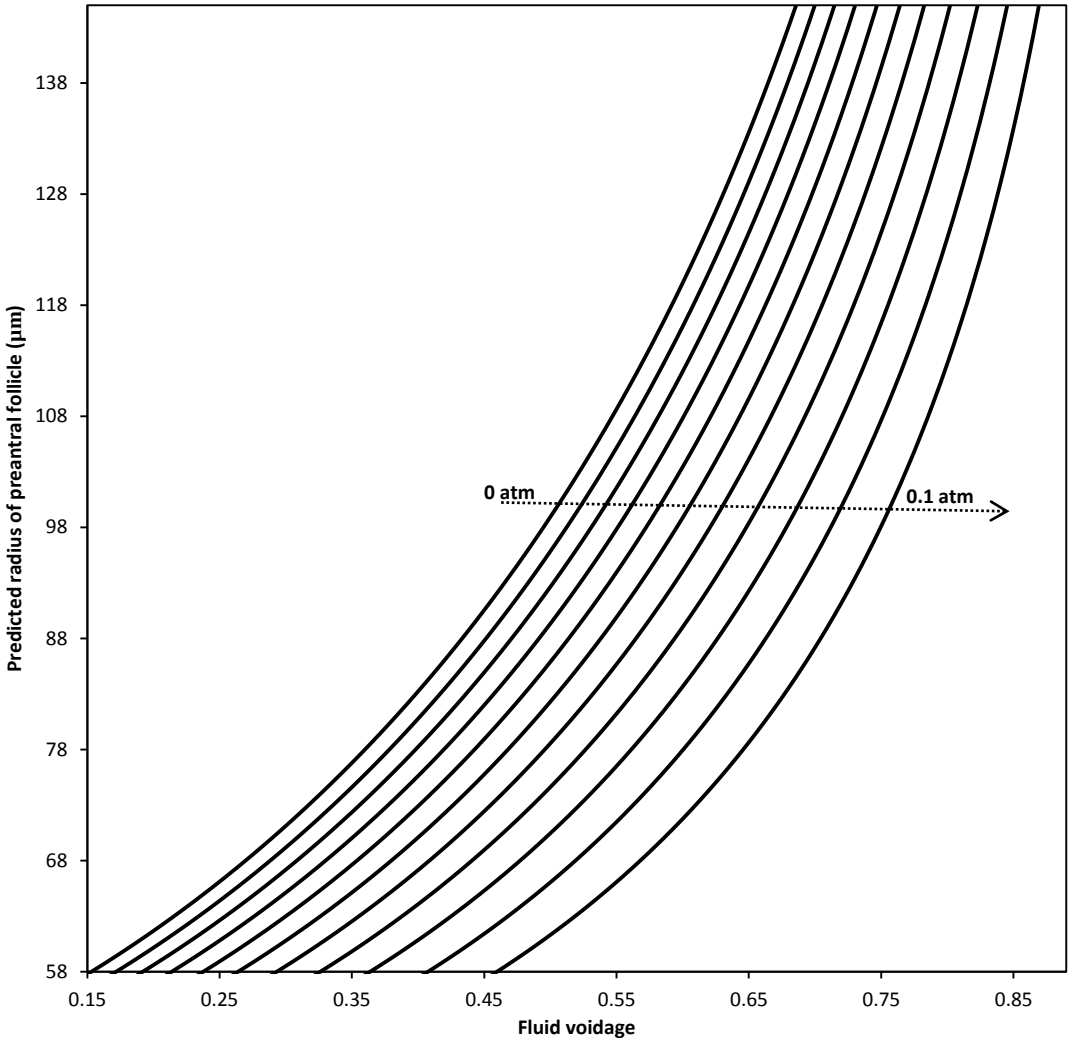

Figure 7.7 A nomograph for determining the maximum follicle radius that can sustain the oocyte at a desired oxygen partial pressure. Where each oxygen level at the oocyte surface from left to right is 0 atm, 0.01 atm, 0.02 atm, 0.03 atm, 0.04 atm, 0.05 atm, 0.06 atm, 0.07 atm, 0.08 atm, 0.09 atm, 0.1 atm respectively. This order is indicated by the arrowhead.

Although not precisely known ideal oxygen levels at the oocyte surface are often suggested as being approximately 0.05 atm. As an example use of Figure 7.7 the maximum follicle size of a follicle which can sustain the oocyte surface at 0.05 atm and has fluid voidage of 0.65 can be read off as approximately 110 µm in radius. Given that a fluid voidage is at maximal levels at a value of 0.65 this can be considered the maximum follicle radius that any follicle can achieve and still oxygenate the oocyte surface at a level of 0.05 atm. Using 0 atm instead shows that the follicle radius beyond which the oocyte will likely experience total hypoxia is approximately 134 µm. This is close to the maximum experimentally observed follicle radius of 145 µm.

It should be stressed that predictions of Figure 7.7 has been carried out at nominal parameter estimate values. Hence they do not account for any of the known variability in these

parameters. As a result, whilst the presented nomogram is a useful tool its results should not be viewed as precise estimates.

7.3 Conclusion

The oxygen consumption rate of granulosa cells determined by this work along with bovine specific parameter estimates have been used to examine oxygen transport in large bovine preantral follicles. The predicted oxygen profiles across the large preantral follicles are consistent with the previous results of Redding *et al.* (2007), which showed that as a preantral follicle grew the oxygen transport across the follicle was increasingly strained, resulting in a gradual decrease in oocyte oxygenation.

The effects of the species specific parameter estimates on the model were demonstrated by comparing predictions made for both bovine and ovine follicles. The results showed that the model was sensitive to the species specific parameter estimates. Specifically, along with the geometric parameters of the model the oxygen consumption rate and fluid voidage of follicles of a given species will be the key determinants in oxygen levels across the follicle.

Furthermore, this work showed that the fluid voidage range across the large bovine preantral follicles was wide and increased as the size of preantral follicles increased. In light of the importance of fluid voidage to oxygen transport, this work suggests that fluid voidage used for predicting the oxygen profile of a large preantral follicle must be specific to the size of the follicle being considered.

Finally a nomograph was produced which allowed prediction of the maximum follicle radius beyond which a given oxygen level at the oocyte surface could no longer be sustained. Such a tool may be useful for examining oxygen transport in follicles across a variety of species.

Chapter 8. Conclusion

This work developed methodology for granulosa cell harvest, culture and subsequent measurements of the oxygen consumption rate of the cells.

The respirometer developed in this work was capable of monitoring oxygen partial pressure in the cell suspension via an optical probe. The respirometer was demonstrated to be able to produce reproducible data and maintain a population of viable cells over the duration of an experimental run.

Five data sets were produced as the result of this experimental work, which allowed this work to analyse the oxygen consumption rate of granulosa cells. The oxygen consumption rate of bovine granulosa cells measured ranged from of 2.1 to 3.3 x 10^{-16}mol.cell^{-1}.s^{-1}/0.16 to 0.25mol.m^{-3}.s^{-1}. This range was comparable with, but higher than cellular oxygen consumption rates in animal cells reported other studies in the literature. In particular the measured rates were approximately 5 times higher than ovine granulosa cells (Gosden & Byatt-Smith 1986).

These oxygen consumption rates were then examined in the context of the oxygen transport in large bovine preantral follicles via an existing mathematic model.

The results showed that the predicted oxygen profiles in large bovine follicles were consistent with the conclusions of Redding *et al.* (2007), which suggested that as a preantral follicle grew the oxygen transport across the follicle was increasingly strained, resulting in a gradual decrease in oocyte oxygenation.

Furthermore, based on the use of the species specific data in the model, this work found that oxygen transport in follicles was likely to be the result of a unique combination of parameters for a particular species. Specifically, in addition to geometric parameters, the oxygen consumption rate and fluid voidage of follicles of a given species would be the key determinants in oxygen levels across the follicle.

This work also found that the fluid voidage range across large bovine preantral follicles was reasonably wide and were higher at larger follicle sizes. This suggested that the use of fluid voidage for investigating the oxygen levels across preantral follicles must be follicle size specific.

Chapter 9. Reference

Alderman J, Hynes J, Floyd SM, Krüger J, O'Connor R, Papkovsky DB. A low-volume platform for cell-respirometric screening based on quenched-luminescence oxygen sensing. Biosensors and Bioelectronics, 19, 1529–1535, 2004.

Allegrucci C, Hunter MG, Webb R, Luck MR. Interaction of bovine granulosa and theca cells in a novel serum-free co-culture system. Reproduction 126 527–538, 2003.

Arain S, John GT, Krause C, Gerlach J, Wolfbeis OS, Klimant I. Characterization of microtiterplates with integrated optical sensors for oxygen and pH, and their applications to enzyme activity screening, respirometry, and toxicological assays. Sensors and Actuators B, 113, 639-648, 2006.

Avery B, Strobech L, Jacobsen T, Bogh IB, Greve T. In vitro maturation of bovine cumulus–oocyte complexes in undiluted FF: effect on nuclear maturation, pronucleus formation and embryo development. Theriogenology, 59, 987–99, 2003.

Barcroft J, Haldane JS. A method of estimating the oxygen and carbonic acid in small quantities of blood. The Journal of Physiology, 28, 232–240, 1902.

Basini G, Bianco F, Grasselli F, Tirelli M, Bussolati S, Tamaninib C. The effects of reduced oxygen tension on swine granulosa cell. Regulatory Peptides, 120, 69–75, 2004.

Basini G, Tamanini C. Selenium stimulates estradiol production in bovine granulosa cells: possible involvement of nitric oxide. Domestic Animal Endocrinology, 18, 1–17, 2000.

Boland NI, Humpherson PG, Leese HJ, Gosden RG. Pattern of lactate production and steroidogenesis during growth and maturation of mouse ovarian follicles in vitro. Biology of Reproduction, 48, 798–806, 1993.

Braems G, Jensen A. Hypoxia reduces oxygen consumption of fetal skeletal muscle cells in monolayer culture. Journal of Developmental Physiology, 16, 209-215, 1991.

Braw-Tal R, Yossefi S. Studies in vivo and in vitro on the initiation of follicle growth in the bovine ovary. Journal of Reproduction and Fertility, 109, 165-171, 1997.

Brown C. Personal communication. School of Engineering and Advanced Technology, Massey Univeristy, Palmerston North, New Zealand.

Calado AM, Rocha E, Colaco A, Sousa M. Stereologic characterization of bovine (*Bos taurus*) cumulus-oocyte complexes aspirated from small antral follicles during diestrous phase. Biology of Reproduction, 65, 1383-1391, 2001.

Castellano FN, Lakowicz JR. A water-soluble luminescence oxygen sensor. Photochemistry and Photobiology, 67, 179-183, 1998.

Cetica P, Pintos L, Dalvit G, Beconi M. Activity of key enzymes involved in glucose and triglyceride catabolism during bovine oocyte maturation in vitro. Reproduction, 124, 657-681, 2002.

Clark AR, Stokes YM, Lane M, Thompson JG. Mathematical modelling of oxygen concentration in bovine and murine cumulus–oocyte complexes. Reproduction, 131, 999–1006, 2006.

Clark AR. Mathematical modelling and experimental investigation of nutrient supply to the mammalian oocyte. Thesis for the degree of philosophy in applied mathematics, University of Adelaide, Adelaide, 2008.

De Castro e Paula LA, Andrzejewski J, Julian D, Spicer LJ, Hansen PJ. Oxygen and steroid concentrations in preovulatory follicles of lactating dairy cows exposed to acute heat stress. Theriogenology, 69, 805–813, 2008.

Donahue RP, Stern S. Follicular cell support of oocyte maturation: production of pyruvate in vitro. Journal of Reproduction and Fertility**,** 17, 395-398, 1968.

Ducommun P, Ruffieux, P, Furter M, Marison I, von Stockar U. A new method for on-line measurement of the volumetric oxygen uptake rate in membrane aerated animal cell cultures. Journal of Biotechnology, 78, 139-147, 2000.

Eppig JJ, Pendola FL, Wigglesworth K, Pendola JK. Mouse oocytes regulate metabolic cooperativity between granulosa cells and oocytes: amino acid transport. Biology of Reproduction**,** 73, 351-357, 2005.

Eppig JJ, Wigglesworth K, Pendola F & Hirao Y. Murine oocytes suppress expression of luteinizing hormone receptor messenger ribonucleic acid by granulosa cells. Biology of Reproduction, 56, 976–984, 1997.

Eutech Instruments Pte Ltd. Dissolved Oxygen Electrodes, 1997. Retrieved from http://www.eutechinst.com/techtips/tech-tips16.htm

Fraser HM. Regulation of the ovarian follicular vasculature. Reproductive Biology and Endocrinology, 4, 2006.

Geva E, Jaffe RB. Role of vascular endothelial growth factor in ovarian physiology and pathology. Elsevier Science Inc, 74, 3, 2000.

Global Environment Centre Foundation. Dissolved Oxygen (DO) Meter, 1997. Retrieved from http://www.gec.jp/CTT_DATA/WMON/CHAP_4/html/Wmon-099.html

Gnaiger E. Oxygen calibration and solubility in experimental media, 2010. Retrieved from http://www.oroboros.at/fileadmin/user_upload/Protocols/MiPNet06.03_O2-Calib-Solubility.pdf

Gosden RG, Byatt-Smith JG. Oxygen concentration gradient across the ovarian follicular epithelium: model, predictions and implications. Human Reproduction, 1, 65-68, 1986.

Gougeon A. Dynamics of follicular growth in the human: a model from preliminary results. Human Reproduction, 1, 81-87, 1986.

Gougeon A. Regulation of ovarian follicular development in primates: facts and hypotheses. Endocrine Reviews, 17, 121-155, 1996.

Hales JRS. Radioactive microsphere measurement of cardiac output and regional tissue blood flow in the sheep. Pflügers Archiv European Journal of Physiology, 344, 119-132, 1973.

Hamberger A, Hamberger L, Larsson S. An automatic recording unit for the micro-diver technique. Experimental Cell Research, 47, 229-236, 1967.

Hamberger L, Hamberger A, Herlitz H. Methods for metabolic studies on isolated granulosa and theca cells. European Journal of Endocrinology, 68, S41-S61, 1971.

Hitchman ML. Measurement of dissolved oxygen. Wiley, New York, 1978

Hynes J, Floyd S, Soini AE, O'Connor R, Papkovsky D. Fluorescence-based cell viability screening assays using water-soluble oxygen probes. Journal of Biomolecular Screening, 8, 2003.

Instech Laboratories. Biological oxygen monitoring systems, 2009. Retrieved from http://www.instechlabs.com/downloads/polarographic.pdf

John GT, Klimant I, Wittmann C, Heinzle E. Integrated optical sensing of dissolved oxygen in microtiter plates: a novel tool for microbial cultivation. Biotechnology and Bioengineering, 81, 829 –836, 2003.

Juengela JL, Sawyerb HR, Smitha PR, Quirkea LD, Heatha DA, Luna S, Wakefieldc SJ, McNattya KP. Origins of follicular cells and ontogony of steroidogenesis in ovine fetal ovaries. Molecular and Cellular Endocrinology, 191, 1–10, 2002.

Kotsuji F, Kamitani N, Goto K, Tominaga T. Bovine Theca and Granulosa Cell Interactions Modulate Their Growth, Morphology, and Function. Biology of Reproduction, 43, 726-732, 1990.

Leese HJ, Barton AM. Production of pyruvate by isolated mouse cumulus cells. Journal of Experimental Zoology, 234, 231-236, 1985.

Li R, Norman RJ, Armstrong DT, Gilchrist RB. Oocyte-secreted factor(s) determine functional differences between bovine mural granulosa cells and cumulus cells. Biology of Reproduction, 63, 839–845, 2000.

Lundy T, Smith P, O'Connell A, Hudson NL, McNatty KP. Populations of granulosa cells in small follicles of the sheep ovary. Reproduction, 115, 251-262, 1999.

Lussier JG, Matton P, Dufour JJ. Growth rates of follicles in the ovary of the cow. Journal of Reproduction and Fertility, 81, 301-307, 1987.

Marieb EN. Human Anatomy & Physiology. 6th ed. San Francisco: Daryl Fox, 2004.

Marion GB, Gier HT, Choudary JB. Micromorphology of the bovine ovarian follicular system. Journal of Animal Science, 27, 451 465, 1968.

Metcalf MG. Estimation of viability of bovine granulosa cells. Journal of Reproduction and Fertility, 65, 425-429, 1982.

Monniaux D, Mariana JC, Gibson WR. Action of PMSG on follicular populations in the heifer. Journal of Reproduction and Fertility, 70, 243-253, 1984.

Moran DT, Rowley JC. Visual Histology, 1988. Retrieved from http://www.columbia.edu/itc/hs/medical/sbpm_histology_old/lab/lab19_micrograph.html

Nandi S, Girish Kumar V, Manjunatha BM, Ramesh HS, Gupta PSP. Follicular fluid concentrations of glucose, lactate and pyruvate in buffalo and sheep, and their effects on cultured oocytes, granulosa and cumulus cells. Theriogenology, 69, 186–196, 2008.

O'Riordan TC, Buckley D, Ogurtsov V, O'Connor R. A Cell viability assay based on monitoring respiration by optical oxygen sensing. Analytical Biochemistry, 278, 221–227, 2000.

Orsi NM, Gopichandran N, Leese HJ, Picton HM, Harris S. Fluctuations in bovine ovarian follicular fluid composition throughout the oestrous cycle. Society for Reproduction and Fertility, 129, 219-228, 2005.

Pawshe CH, Appa Rao KBC, Totey SM. Effect of insulin-like growth factor I and its interaction with gonadotropins on in vitro maturation and embryonic development, cell proliferation, and biosynthetic activity of cumulus-oocyte complexes and granulosa cells in buffalo. Molecular reproduction and development, 49, 277-285, 1998.

Peterson JI, Fitzgerald RV, Buckhold DK. Fiber-optic probe for in vivo measurement of oxygen partial pressure. Analytical Chemistry, 56, 62–67, 1984.

Picton H, Briggs D, Gosden R. The molecular basis of oocyte growth and development. Molecular and Cellular Endocrinology, 145, 27–37, 1998.

Rank Brothers Ltd. The Rank Brothers Oxygen Electrode Operating Manual, 2002. Retrieved from http://www.rankbrothers.co.uk/prod1.htm

Redding GP, Bronlund JE, Hart AL. Mathematical modelling of oxygen transport-limited follicle growth. Reproduction, 133, 1095–1106, 2007.

Redding GP, Bronlund JE, Hart AL. Theoretical investigation into the dissolved oxygen levels in follicular fluid of the developing human follicle using mathematical modelling. Reproduction, Fertility and Development, 20, 408–417, 2008.

Redding GP. Oxygen and ovarian follicle. Thesis for degree of Doctor of Philosophy in Bioprocess Engineering, Massey University, Palmerston North, New Zealand, 2007.

Redding GP. Personal communication. School of Engineering and Advanced Technology, Massey Univeristy, Palmerston North, New Zealand.

Riley MR, Muzzio FJ, Buettner HM, Reyes SC. A simple - correlation for predicting effective diffusivities in immobilized cell systems. Biotechnology and Bioengineering, 49, 223-227, 1996.

Riley MR, Muzzio FJ, Buettner HM, Reyes SC. Diffusion in heterogeneous media: application to immobilized cell systems. AIChE Journal. 41, 691-700, 1995.

Riley MR, Muzzio FJ, Buettner HM, Reyes SC. Monte carlo calculation of effective diffusivities in two- and three- dimensional heterogeneous materials of variable structure. American Journal of Physiology, 49, 3500-3503, 1994.

Ruffieux P, von Stockar U, Marison IW. Measurement of volumetric (OUR) and determination specific (pO_2) oxygen uptake rates in animal cell cultures. Journal of Biotechnology, 63, 85-95, 1998.

Salha O, Abusheika N, Sharma V. Dynamics of human follicular growth and in vitro oocyte maturation. Human Reproduction Update, 4, 816–32, 1998.

Shier D, Butler J, Ricki L. Hole's Essentials of Human Anatomy and Physiology. 9th ed, New York: McGraw-Hill, 2006.

Slininger PJ, Petroski RJ, Bothast RJ. Measurement of oxygen solubility in fermentation media: a colorimetric method. Biotechnology and Bioengineering, 33, 578-583, 1989.

Sugiura K, Eppig JJ. Control of metabolic cooperativity between oocytes and their companion granulosa cells by mouse oocytes. Developmental biology, 17, 667-674, 2005.

Sugiura K, Pendola FL, Eppig JJ. Oocyte control of metabolic cooperativity between oocytes and companion granulosa cells: energy metabolism. Developmental Biology, 279, 20–30, 2005.

Sutton ML, Cetica PD, Beconi MT, Kind KL, Gilchrist RB, Thompson JG. Influence of oocyte-secreted factors and culture duration on the metabolic activity of bovine cumulus cell complexes. Reproduction, 126, 27–34, 2003.

Telfer EE. The development of methods for isolation and culture of preantral follicles from bovine and porcine ovaries. Thenogenology, 45, 101-110, 1996.

Truskey GA, Yuan F, Katz DF. Transport in porous media. New Jersey: Pearson Prentice Hall, 2004.

University of Leeds. Oxygen electrodes, 2010. Retrieved from http://www.bmb.leeds.ac.uk/illingworth/oxphos/electrod.htm

Van Blerkom J, Antczak M, Schrader R. The developmental potential of the human oocyte is related to the dissolved oxygen content of follicular fluid: association with vascular endothelial growth factor levels and perifollicular blood flow characteristics. Human Reproduction, 12, 1047–1055, 1997.

Van den Hurk R, Zhao J. Formation of mammalian oocytes and their growth, differentiation and maturation within ovarian follicles. Theriogenology, 63, 1717–1751, 2005.

Vanderhyden BC, Telfer EE, Eppig JJ. Mouse oocytes promote proliferation of granulosa cells from preantral and antral follicles in vitro. Biology of Reproduction, 46, 1196-1204, 1992.

Wagner AE, Muir WW, Grospitch BJ. Cardiopulmonary effects of position in conscious cattle. American Journal of Veterinary Research, 51, 7-10, 1990.

Warburg O, Wind F, Negelein E**.** Über den Stoffwechsel von Tumoren im Körper. Journal of Molecular Medicine, 5, 829-832, 1926 (English translation by Dickens F 1930 Constable London).

Yada H, Hosokawa K, Tajima K, Hasegawa Y, Kotsuji F. Role of ovarian theca and granulosa cell interaction in hormone production and cell growth during the bovine follicular maturation process. Biology of Reproduction, 61**,** 1480–1486, 1999.

Yang MY, Rajamahendran R. Morphological and biochemical identification of apoptosis in small, medium, and large bovine follicles and the effects of follicle-stimulating hormone and insulin-like growth factor-I on spontaneous apoptosis in cultured bovine granulosa cells. Biology of Reproduction, 62, 1209–1217, 2000.